

Non-Coding Genetic Analysis Implicates Interleukin 18 Receptor Accessory Protein 3'UTR in Amyotrophic Lateral Sclerosis

Authors:

Chen Eitan¹, Elad Barkan², Tsviya Olender¹, Kristel R. van Eijk³, Matthieu Moisse^{4,5}, Sali M. K. Farhan^{6,7}, Aviad Siany¹, Shu-Ting Hung⁸⁻¹⁰, Nancy Yacovzada^{1,2}, Johnathan Cooper-Knock¹¹, Kevin P. Kenna³, Rick A. A. van der Spek³, William Sproviero¹², Ahmad Al Khleifat¹², Alfredo Iacoangeli¹², Aleksey Shatunov¹², Ashley R. Jones¹², Elik Chapnik¹, Daphna Rothschild^{2,13,14}, Omer Weissbrod², Sebastian Werneburg¹⁵, Dorothy P. Schafer¹⁵, Robert H. Brown Jr¹⁶, Pamela J. Shaw¹¹, Philip Van Damme^{4,5,17}, Leonard H. van den Berg³, Hemali P. Phatnani¹⁸, Eran Segal², Justin K. Ichida⁸⁻¹⁰, Ammar Al-Chalabi^{12,19}, Jan H. Veldink³, Project MinE ALS Sequencing Consortium²⁰, NYGC ALS Consortium²⁰ and Eran Hornstein^{1*}

Affiliations:

¹Department of Molecular Genetics, Weizmann Institute of Science, Rehovot 7610001, Israel.

²Department of Computer Science And Applied Math, Weizmann Institute of Science, Rehovot 7610001, Israel.

³Department of Neurology, UMC Utrecht Brain Center, University Medical Center Utrecht, Utrecht University, Utrecht, 3584 CG, The Netherlands.

⁴KU Leuven - University of Leuven, Department of Neurosciences, Experimental Neurology, B-3000 Leuven, Belgium.

⁵VIB, Center for Brain & Disease Research, Laboratory of Neurobiology, Leuven, Belgium.

⁶Analytic and Translational Genetics Unit, Center for Genomic Medicine, Massachusetts General Hospital and Harvard Medical School, Boston, MA 02114, USA.

⁷Stanley Center for Psychiatric Research, Broad Institute of MIT and Harvard, Cambridge, MA 02142, USA.

⁸Department of Stem Cell Biology and Regenerative Medicine, Keck School of Medicine, University of Southern California, Los Angeles, CA 90033, USA.

⁹Eli and Edythe Broad CIRM Center for Regenerative Medicine and Stem Cell Research at USC, Los Angeles, CA 90033, USA.

¹⁰Zilkha Neurogenetic Institute, Keck School of Medicine of the University of Southern California, Los Angeles, CA 90033, USA.

¹¹Sheffield Institute for Translational Neuroscience (SITraN), University of Sheffield, Sheffield S10 2HQ, UK.

¹²King's College London, Maurice Wohl Clinical Neuroscience Institute, Institute of Psychiatry, Psychology & Neuroscience, De Crespigny Park, London, SE5 8AF, United Kingdom.

¹³Department of Developmental Biology, Stanford University, Stanford, CA 94305, USA

¹⁴Department of Genetics, Stanford University, Stanford, CA 94305, USA

¹⁵Department of Neurobiology, Brudnick Neuropsychiatric Research Institute, University of Massachusetts Medical School, Worcester, MA 01605, USA.

¹⁶Department of Neurology, University of Massachusetts Medical School, Worcester, MA 01655, USA.

¹⁷University Hospitals Leuven, Department of Neurology, Leuven, Belgium.

¹⁸Center for Genomics of Neurodegenerative Disease, New York Genome Center.

¹⁹King's College Hospital, Denmark Hill, London, SE5 9RS, United Kingdom.

²⁰A list of Consortiums PIs and affiliations appears in the Supplementary Information.

*Corresponding author. Tel: +972 89346215; Fax: +972 89342108; E-mail: Eran.hornstein@weizmann.ac.il

Abstract:

The non-coding genome is substantially larger than the protein-coding genome, but the lack of appropriate methodologies for identifying functional variants limits genetic association studies. Here, we developed analytical tools to identify rare variants in pre-miRNAs, miRNA recognition elements in 3'UTRs, and miRNA-target networks. Region-based burden analysis of >23,000 variants in 6,139 amyotrophic lateral sclerosis (ALS) whole-genomes and 70,403 non-ALS controls identified Interleukin-18 Receptor Accessory Protein (IL18RAP) 3'UTR variants significantly enriched in non-ALS genomes, replicate in an independent cohort and associate with a five-fold reduced risk of developing ALS. IL18RAP 3'UTR variants modify NF- κ B signaling, provide survival advantage for cultured ALS motor neurons and ALS patients, and reveal direct genetic evidence and therapeutic targets for neuro-inflammation. This systematic analysis of the non-coding genome and specifically miRNA-networks will increase the power of genetic association studies and uncover mechanisms of neurodegeneration.

One Sentence Summary: Non-coding genetics demonstrate rare variants in IL-18 receptor 3'UTR that modifies ALS risk and progression.

1 **[Main Text:]**

2 **Introduction**

3 Genomic sequencing technologies facilitate identification of variants in open reading frames (ORFs).
4 Although allelic variants in non-coding regions are expected to be numerous ^{1, 2} they are largely
5 overlooked because current analytical approaches do not adequately prioritize variants that are likely to
6 be functional, over neutral background variation.

7 Amyotrophic lateral sclerosis (ALS) is a fatal neurodegenerative syndrome, primarily affecting the human
8 motor neuron system with a strong genetic predisposing component ^{3, 4}. Thus, mutations in approximately
9 25 protein-coding genes have been associated with ALS ^{3, 5, 6} and a hexanucleotide repeat expansion in an
10 intronic sequence of the *C9orf72* gene is the most common genetic cause of ALS ⁷⁻⁹. However, non-coding
11 nucleotide variants in ALS have yet to be systematically explored.

12 MicroRNAs (miRNAs) are endogenous posttranscriptional repressors that silence mRNA expression
13 through sequence complementarity. miRNA dysregulation has been implicated in ALS pathogenesis, and
14 ALS-associated RNA-binding proteins, *TARDBP*/TDP-43 and *FUS*, regulate miRNA biogenesis ¹⁰⁻²¹.
15 miRNA primarily act on 3' untranslated regions (3'UTRs) ²², which are non-coding parts of messenger
16 RNAs (mRNAs) and often regulate degradation and translation ²³.

17 Burden analysis is a genetics approach that is based on the rationale that different rare variants in the same
18 gene may have a cumulative contribution ²⁴. Therefore, burden analysis allows the identification of genes
19 containing an excess of rare and presumably functional variation in cases relative to controls. Although
20 de novo mutations in non-coding regions were recently shown in family-based autism studies ²⁵, variants
21 in non-coding regions are not routinely included in rare-variant burden association studies. The application
22 of burden analysis to non-coding regulatory variation is constrained by the availability of whole genome
23 sequencing (WGS) data, and the ability to recognize functional variants in non-coding regulatory regions,
24 which is currently far less effective than for protein-coding genes.

25 To effectively apply burden analyses to regulatory variation, appropriate ways to determine what are the
26 relevant (qualifying) variants should be determined. In the case of miRNAs and miRNA recognition
27 elements such a framework can be achieved with relatively high confidence because of miRNA high

28 conservation and wealth of mechanistic insight about sequence impact on function. Therefore, miRNA
29 regulatory networks make an excellent gene set to explore.

30 Here, we developed tools that identify, or call, qualifying variants in miRNAs and 3'UTR of mRNAs, and
31 performed collapsed genetic analysis ²⁶, to test if these regulatory RNAs are associated with ALS. We
32 discovered an enrichment of rare variants in the IL18RAP 3'UTR, implicating the IL-18 pathway in ALS.
33 Non-coding variants analysis in miRNA networks may impact research of human traits, increase the power
34 of rare-variant association methods and encourage systematic exploration of non-coding regions, to
35 uncover genetic mechanisms of disease.

36 Results

37 To test whether genetic variations in non-coding regulatory regions are associated with ALS, we analyzed
38 regions of interest WGS data from the Project MinE ALS sequencing consortium ²⁷ ([Supplementary Fig.
39 1A,B and Supplementary Tables 1,2](#)). The discovery cohort consisted of 3,955 ALS patients and 1,819 age-
40 and sex-matched controls, for a total of 5,774 whole-genomes from the Netherlands, Belgium, Ireland,
41 Spain, United Kingdom, United States and Turkey (Project MinE Datafreeze 1). We tested 295 genes,
42 including candidates from sporadic ALS GWAS ²⁸ or encoding RNA-binding proteins, and analyzed both
43 their 3'UTRs and open reading frames ([Supplementary Table 3](#)). In addition, we tested all 1,750 human
44 precursor miRNA genes (pre-miRNAs; miRBase v20) ²⁹.

45 We devised a method for identifying rare genetic variants with minor allele frequencies (MAF) ≤ 0.01 , in
46 non-coding RNA regulation that: (1) abrogate miRNA recognition elements in 3'UTRs; or (2) result in a
47 predicted *de novo* gain of miRNA binding; or (3) change the sequence of mature miRNAs and/or pre-
48 miRNAs (miRBase v20²⁹). We performed region-based burden test, in which variants within miRNA
49 recognition elements in 3'UTRs and within pre-miRNA genes that satisfy above criteria (qualifying
50 variants), were binned together to weight their contribution to disease.

51 We also identified rare variants in open reading frame of the 295 miRNA-relevant or ALS-relevant protein
52 coding genes, that are predicted to cause frameshifting, alternative splicing, an abnormal stop codon, or a
53 deleterious non-synonymous amino acid substitution that were detected in ≥ 3 of 7 independent dbNSFP
54 prediction algorithms ³⁰ ([Fig. 1A and Supplementary Table 3](#)). In total 28,211 rare qualifying variants
55 were identified ([Supplementary Table 4](#)).

56 As positive control we performed an association analysis of rare variants in protein-coding sequences,
57 using the Optimized Sequence Kernel Association Test (SKAT-O) ³¹. SKAT-O identified a significant
58 excess of deleterious minor alleles in the ALS genes *NEK1* (127 cases; 19 controls [3.21%; 1.04%]: $P =$
59 7.04×10^{-7} ; $P_{corrected} = 2.13 \times 10^{-4}$), comparable with a reported prevalence of 3% ³², and *SOD1* (36 cases
60 [0.91%]; 0 controls: $P = 2.61 \times 10^{-4}$; $P_{corrected} = 3.76 \times 10^{-2}$) ³³, which is below the reported 2% prevalence ⁵.
61 ³⁴ ([Fig. 1B, Supplementary Fig. 2A and Data File S1](#)). Other known ALS genes did not reach statistical
62 significance ([Supplementary Table 3](#)), consistent with reported statistical power limitations of Project
63 MinE WGS data in assessing the burden of rare variants ³⁵. Our analysis did not consider *C9orf72*
64 hexanucleotide (GGGGCC) repeat expansion region.

65 We determined the burden of rare variants in all autosomal pre-miRNAs in the human genome (1,750
66 genes). We did not identify disease association for any pre-miRNAs, nor for any of the predicted genetic
67 networks based on variants aggregated over specific mature miRNAs and their cognate downstream
68 3'UTR targets. This may be because the small size of miRNA genes makes genetic aggregation studies
69 particularly challenging (Supplementary Fig. 2B,C).

70 Finally, we tested the burden of variants that are potentially either abrogating conserved miRNA binding
71 sites or creating new miRNA binding sites in 3'UTRs. The strongest association was for the 3'UTR of
72 *IL18RAP* (Fig. 1B, Supplementary Fig. 2D and Data File S1). This association was higher than expected
73 at random ($P = 3.34 \times 10^{-5}$, $P_{corrected} = 9.31 \times 10^{-3}$) and from the association gained for all protein-coding
74 ALS genes in this cohort, with the exception of *NEK1*. Notably, the signal was more prevalent in controls
75 [9/1819, 0.49%] relative to ALS patients [4/3955, 0.10%], indicating that these variants are protective
76 against ALS.

77 Because the number of ALS genomes was ~2.17-fold larger than the number of controls, the data depict
78 a 4.89-fold enrichment in the abundance of variants in controls over cases. *IL18RAP* 3'UTR protective
79 variants reduced the disease odds ratio by five-fold (OR = 0.20; Fig. 2A), and was consistent across
80 independent population strata (Fig. 2B), whereas *NEK1* and *SOD1* increased the disease odds ratio (OR =
81 3.14, 33.89, respectively; Fig. 2A).

82 *IL18RAP* 3'UTR also ranked as the top hit when we relaxed the analysis by including all 3'UTR variants,
83 regardless of predicted miRNA recognition elements. Therefore, the robust association of *IL18RAP*
84 3'UTR is independent of the assumptions about specific miRNA binding (SKAT-O $P = 1.88 \times 10^{-5}$, $P_{corrected}$
85 $= 5.62 \times 10^{-3}$; variant in controls [12/1819, 0.66%], cases [6/3955, 0.15%], OR = 0.23; Fig. 2A,C, Fig. 3A,
86 Supplementary Table 5 and Data File S1). Three other algorithms – the Sequence Kernel Association Test
87 (SKAT, $P = 1.73 \times 10^{-5}$; permuted P-value $< 10^{-4}$), the Combined Multivariate and Collapsing (CMC, P
88 $= 8.66 \times 10^{-4}$) or Variable Threshold (VT) with permutation analysis (permuted P-value $= 2.10 \times 10^{-3}$) –
89 all ranked the *IL18RAP* 3'UTR association above any other studied 3'UTR, suggesting that the association
90 does not depend on a particular statistical genetics method (Supplementary Fig. 3). Together, rare variants
91 in *IL18RAP* 3'UTR are depleted in ALS patients, suggesting that they are protective against ALS.

92 To determine if the rare *IL18RAP* 3'UTR variants are depleted in another ALS cohort, we performed
93 independent replication studies. Similar results for rare *IL18RAP* 3'UTR variants were reproduced in the

94 New York Genome Center (NYGC) ALS Consortium cohort (2,184 ALS genomes), which was studied
95 against: (i) 263 non-neurological controls from the NYGC; (ii) 62,784 non-ALS genomes from NHLBI's
96 Trans-Omics for Precision Medicine (TOPMed); and (iii) 5,537 non-ALS genomes from gnomAD. This
97 replication effort yielded a joint analysis P-value = 9.58×10^{-4} (χ^2 with Yate's correction; OR=0.32; 95%
98 CI: 0.16 – 0.64; [Fig. 2C and Supplementary Table 6](#)). Combining this cohort with our discovery cohort
99 from Project MinE, yielded a superior joint P-value < 1.00×10^{-5} (χ^2 with Yate's correction; OR=0.20;
100 95% CI: 0.12 – 0.34; [Fig. 2C](#)). A meta-analysis of Project MinE datafreeze 1 and 2, which consisted of
101 5,185 ALS patients and 2,262 age- and sex-matched controls, reproduced the initial signal ($p = 7.6 \times 10^{-4}$).

102 Together, *IL18RAP* 3'UTR sequence variants contribute to a lower risk of suffering from ALS, that is
103 approximately one fifth of the general population, although it did not reach conventional exome-wide
104 multiplicity-adjusted significance threshold ($\alpha \approx 2.6 \times 10^{-6}$, ref. ²⁴) in our study.

105 Finally, genome-wide analysis of all known human 3'UTRs (RefSeq, ³⁶) identified *IL18RAP* 3'UTR as
106 the most significant 3'UTR associated with ALS, in the Project MinE cohort ([Fig. 3B](#)), followed by the
107 *GPATCH8* 3'UTR (SKAT-O P = 1.92×10^{-5} , $P_{corrected} = 0.16$; variant in controls [63/1819, 3.46%], cases
108 [68/3955, 1.72%], OR = 0.49), the *CDC14B* 3'UTR (SKAT-O P = 3.64×10^{-5} , $P_{corrected} = 0.19$; variant in
109 controls [112/1819, 6.16%], cases [163/3955, 4.12%], OR = 0.66), and the *RAB3GAP2* 3'UTR (SKAT-O
110 P = 4.51×10^{-5} , $P_{corrected} = 0.19$, variant in controls [147/1819, 8.08%], cases [485/3955, 12.26%], OR =
111 1.59). *GPATCH8* is involved in hyperuricemia pathophysiology, *CDC14B* is a dual-specificity
112 phosphatase involved in the DNA damage response, and *RAB3GAP2* is involved in neurotransmitter and
113 hormone exocytosis and highly expressed in the brain, however, their potential role in neurodegeneration
114 is unknown.

115 To investigate the source of the signal in the *IL18RAP* 3'UTR in a post-hoc analysis, we divided the 11
116 variant nucleotides into two synthetic sets, of either nine singleton variants (9 variants / 3 controls / 6
117 patients) or two variants that were identified solely in controls (2 variants / 9 controls / 0 patients). While
118 the signal of the nine singleton variants was not statistically significant, analysis of the two control
119 variants, which were identified in multiple samples, derived an improved significance compared to the
120 original signal (SKAT-O P = 4.36×10^{-6}). Thus, these two rare variants (V1, Chr2:103068691 C>T; V3,
121 Chr2:103068718 G>A) are likely central in generating the genetic association signal in *IL18RAP* 3'UTR.

122 IL18RAP is a receptor subunit which dimerizes with IL18R1 upon binding of the interleukin IL-18. IL18
123 receptor is expressed in T-cells, neurons, astrocytes, and microglia³⁷ and induces NF- κ B signaling. To
124 determine the functional impact of the *IL18RAP* variants we analyzed *IL18RAP* expression in
125 lymphoblastoid cell lines (LCLs) from the UK MNDA DNA Bank³⁸ that were originally derived from
126 two different individuals, one carrying the putative *IL18RAP* protective variant (V3, Chr2:103068718
127 G>A) and the other carrying the canonical *IL18RAP* 3'UTR (control). LCLs harboring the *IL18RAP*
128 3'UTR protective variant significantly down-regulated IL18RAP protein expression (Fig. 4A and Data
129 File S2), with p-NF- κ B protein levels also being significantly reduced (Fig. 4B and Data File S3).
130 Therefore, a variant form of *IL18RAP* 3'UTR attenuates its endogenous expression and downstream NF-
131 κ B signaling.

132 To further establish the functional relevance of the *IL18RAP* 3'UTR variants, we subcloned wild-type
133 *IL18RAP* 3'UTR (WT) and the two most prevalent 3'UTR variants, (Chr2:103068691 C>T (V1) and
134 Chr2:103068718 G>A (V3)), downstream of a Renilla luciferase reporter (hRluc). Variants V3 and V1
135 reduced luciferase activity by ~33% and ~30%, respectively, relative to the WT *IL18RAP* 3'UTR (Fig.
136 4C,D). Thus, the protective *IL18RAP* variants regulate *IL18RAP* mRNA expression.

137 To determine the ability of the *IL18RAP* variants V3 and V1 to induce NF- κ B activity, we co-transfected
138 U2OS cells with different *IL18RAP* coding region (CDS) and 3'UTR constructs, along with an NF- κ B
139 activity reporter that drives luciferase (Luc2P) transcription via five copies of the NF- κ B response
140 element. NF- κ B signaling was induced by adding a human recombinant IL-18 to the medium. Variants
141 V3 and V1 of the *IL18RAP* 3'UTR reduced NF- κ B activity by ~10% and ~21%, respectively, relative to
142 the WT *IL18RAP* 3'UTR (Fig. 4E,F). GFP vector and a dominant negative coding mutant E210A-Y212A-
143 Y214A CDS + WT 3'UTR (3CDS)³⁹, served as controls. We conclude that V3 and V1 3'UTR variants
144 affect IL18RAP capacity to induce NF- κ B signaling, although physiological relevance cannot be
145 elucidated from a reporter assay.

146 Levels of the cytokine IL-18 are elevated in ALS patient tissues and biofluids⁴⁰⁻⁴², but the expression in
147 motor neurons is not characterized. To study *IL-18* and *IL18RAP* expression levels specifically in human
148 motor neurons of patients with ALS, we mined human NGS data. *IL18RAP* and *IL-18* mRNA expression
149 are higher in laser capture microdissection– enriched surviving motor neurons from lumbar spinal cords
150 of patients with sALS with rostral onset and caudal progression, relative to non-neurodegeneration
151 controls (Supplementary Fig. 4A,B; data from ref.⁴³). Consistently, higher *IL-18* mRNA levels were also

152 in induced human motor neurons of patients with ALS (Supplementary Fig. 4C; data from ref. 44)). Thus,
153 *IL-18* and *IL18RAP* receptor subunit are abnormally high in human ALS motor neurons.

154 To study the impact of *IL18RAP* 3'UTR mutations in a model of human ALS motor neurons, we
155 performed a survival analyses using induced pluripotent stem cells (iPSCs) derived from human ALS
156 patients that harbor a *C9orf72* hexanucleotide repeat expansion⁴⁵. iPSCs from patients and from healthy
157 controls were differentiated to Hb9::RFP+ human motor neurons (iMNs)⁴⁵ and time-lapse microscopy
158 was used to quantify their subsequent survival after withdrawal of neurotrophic factors and in the presence
159 of the cytokine IL-18 (Fig. 5A). As expected, degeneration (cellular death) was significantly more severe
160 in *C9orf72* patient iMNs than in iMNs derived from healthy controls (n=2 patients, n=2 controls, iMNs
161 from each genotype combined into a single trace for clarity; Fig. 5B). Notably, this was partially rescued
162 by transducing *C9orf72* iPSCs with the *IL18RAP* 3'UTR variant V3 (including CDS) expression vector,
163 which ameliorated motor neuron toxicity, relative to wild-type *IL18RAP* 3'UTR. This was similar to the
164 effect of a *IL18RAP* dominant negative coding mutant, 3CDS (E210A-Y212A-Y214A; one-sided log-
165 rank test, P<0.05, n=2 patients, n=2 controls, Fig. 5B-D). The V1 variant had a more limited effect, which
166 might be related to activity of V1 in cells other than motor neurons. Additionally, *C9orf72* iMNs harboring
167 the V3 variant displayed a lower hazard ratio (cellular death propensity) than *C9orf72* iMNs harboring
168 the wild-type *IL18RAP* 3'UTR, (n=2 patients, n=2 controls (Fig. 5E). Thus, both IL18RAP and its ligand
169 IL-18 are upregulated in human ALS motor neurons and a rare variant of *IL18RAP* 3'UTR confers
170 protection to human *C9orf72* motor neurons in tissue culture.

171 To determine whether the mutant *IL18RAP* 3'UTR is also protective in human patients with ALS, we
172 tested the association between age of diagnosis and age of death in ALS patients harboring wild-type or
173 variants of the *IL18RAP* 3'UTR. Of 4216 patients for whom data on age of diagnosis was available
174 (Project MinE and NYGC cohorts), 8 harbored *IL18RAP* 3'UTR variants. Of 4263 patients for whom age
175 of death was available, 9 harbored *IL18RAP* 3'UTR variants. *IL18RAP* variants are expected to be
176 depleted in ALS genomes, nonetheless in those extremely rare patients harboring *IL18RAP* 3'UTR
177 variants, these were associated with an older age of death, on average 6.1 years after the average for
178 patients with canonical *IL18RAP* 3'UTR (one-sided Mann-Whitney test P = 0.037; Fig. 5F), and an older
179 age of diagnosis, on average 6.2 years after the average for patients with canonical *IL18RAP* 3'UTR (one-
180 sided Mann-Whitney test P = 0.06; Fig. 5G). Thus, variants in *IL18RAP* 3'UTR are protective against
181 ALS and provide survival advantage for patients suffering from the disease.

182 Discussion

183 Data from the ALS consortia used in this study, Project MinE and NYGC, provide unprecedented
184 opportunities for investigating the role of the non-coding genome in ALS, and will drive the development
185 of computational methodologies for weighting the effect of variants outside of protein open reading
186 frames. By identifying qualifying variants and performing rare variant aggregation analysis in 1,750 pre-
187 miRNA genes, and 295 protein coding ORFs and their 3'UTRs, we demonstrated that variants in the
188 3'UTR of *IL18RAP* are enriched in non-ALS genomes, indicating that these are relatively depleted in
189 ALS. *IL18RAP* 3'UTR variants reduced the chance of the disease five-fold, increased the survival of
190 human *C9orf72* motor neurons and delayed onset and therefore age of death in people with ALS. The
191 discovery of functional, disease-modifying *IL18RAP* 3'UTR variants underscores the need to explore the
192 role of additional non-coding genomic regions in ALS.

193

194 Protective protein-coding variants have been identified in Alzheimer's disease⁴⁶⁻⁴⁹ and implicated in ALS
195 as well^{50, 51} and deleterious variants were suggested in VEGF promoter/5'UTR⁵². However, the 3'UTR
196 of *IL18RAP* is the first protective non-coding allele associated with a neurodegenerative disease.

197

198 Neuro-inflammation is prevalent in neurodegeneration, including in ALS⁵³, and is often characterized by
199 the activation of microglia, astrocytes, and the accumulation of infiltrating T-cells at sites of
200 neurodegeneration⁵⁴⁻⁵⁷. The soluble ligand, IL-18, is part of this neuro-inflammatory milieu, promoting
201 receptor subunit (IL18RAP, IL18R1) dimerization on the membrane of T-cells, neurons, astrocytes, and
202 microglia³⁷, and activating intracellular signaling cascades, including NF- κ B. Polymorphic forms of
203 IL18RAP are genetically associated with autoimmune / inflammatory diseases⁵⁸⁻⁶², suggesting that
204 perhaps changes to IL18RAP via its 3'UTR, alter ALS risk or severity in a dose or expression-dependent
205 manner.

206

207 Our study directly links dysregulation of IL18RAP signaling to ALS. The protective effect of IL18RAP
208 3'UTR variants causes downregulation of IL-18 signaling, which might be hyperactive in ALS motor
209 neurons and is supported by previous observations showing that ALS patients have elevated levels of the
210 cytokine IL-18 in tissues and biofluids⁴⁰⁻⁴² and that IL-18 secretion is triggered from microglia in a model
211 of TDP-43 proteinopathy⁶³. Our data from human motor neurons further suggest that IL18RAP may be
212 acting directly on motor neurons. Therefore, variants in *IL18RAP* 3'UTR may modify IL-18 signaling in

213 the central nervous system of ALS patients. However, the regulatory changes affected by the *IL18RAP*
214 3'UTR variants remains to be elucidated.

215

216 A limitation of our study is that only 295 candidate genes were initially tested. However, the key findings
217 were reproduced in a genome-wide study of all human 3'UTRs. While *IL18RAP* 3'UTR signal is
218 comparable to that of protein-coding ALS-causing genes, such as *SOD1* and *NEK1*, limitations in the
219 statistical power may be overcome with larger ALS and control cohorts, which are not currently available.
220 Furthermore, the genetic involvement of *IL18RAP* 3'UTR in other neurodegenerative diseases remains to
221 be explored. Finally, the mechanism underlying *IL18RAP* dose sensitivity is not fully understood. While
222 we provide evidence that *IL18RAP* 3'UTR endows neuroprotection to human motor neurons and is
223 associated with survival advantage in humans with ALS, additional studies should explore the mechanism
224 by which *IL18RAP* protects motor neurons and the degree to which other cell types, such as microglia,
225 are involved.

226

227 In summary, we have identified the *IL18RAP* 3'UTR as a non-coding genetic disease modifier by burden
228 analysis of WGS data using ALS case-control cohorts. We show that IL-18 signaling modifies ALS
229 susceptibility and progression, delineating a neuro-protective pathway and identifying potential
230 therapeutic targets for ALS. Whereas the 3'UTR of *IL18RAP* is the first protective non-coding allele
231 associated with a neurodegenerative disease, the increasing wealth of WGS data in Project MinE, NYGC
232 and elsewhere, indicates that the exploration of non-coding regulatory genomic regions should reveal
233 further disease-relevant genetic mechanisms.

234 **Methods**

235

236 **Human genetic cohorts**

237 All participants contributed DNA after signing informed consent at the submitting sites. Human materials
238 were studied under approval of the Weizmann Institute of Science Institutional Review Board (Weizmann
239 IRB: 1039-1).

240 Discovery cohort: Project MinE ALS sequencing consortium Datafreeze 1 includes 3,955 ALS patients
241 and 1,819 age- and sex-matched controls, free of any neurodegenerative disease, for a total of 5,774 quality
242 control (QC) passing whole-genomes, from the Netherlands, Belgium, Ireland, Spain, United Kingdom,
243 United States and Turkey. Rare variant association in cases versus controls was evaluated for regions of
244 interest, when we could identify ≥ 2 variants per region, by SKAT-O, SKAT, CMC and VT in RVTESTS
245 environment⁶⁴, with sex and the top 10 principal components (PCs) as covariates. To construct the PCs
246 of the population structure, an independent set of $\sim 450,000$ SNPs was sampled from WGS, ($MAF \geq 0.5\%$)
247 followed by LD-pruning.

248 Replication cohorts: Utilized for testing rare variant alleles ($MAF < 0.01$) in human *IL18RAP* 3'UTR
249 (GRCh37/hg19 chr2:103068641-103069025 or GRCh38 chr2:102452181-102452565) from Project
250 MinE datafreeze 2: ~ 1300 European heritage ALS genomes without middle eastern (Turkish and Israelis)
251 genomes. The New York Genome Center (NYGC) ALS Consortium (2,184 ALS Spectrum MND and 263
252 non-neurological control genomes from European/Americas ancestries), NHLBI's Trans-Omics for
253 Precision Medicine (TOPMed; 62,784 non-ALS genomes) and gnomAD (5,537 non-ALS genomes;
254 Europeans, non-Finnish, non-TOPMed). Joint analysis in replication cohort, was performed by Chi square
255 test with Yate's correction. Meta-analysis was not possible because TOPMed and gnomAD covariate
256 information is not available.

257 **Quality control procedures in Project MinE genomics**

258 Sample selection, data merging and sample- and variant level quality control procedures for Project MinE
259 ALS sequencing consortium genomes are described in full previously³⁵. Briefly, 6,579 Project MinE ALS
260 sequencing consortium whole genomes sequenced on Illumina HiSeq2000 or HiSeqX platforms. Reads
261 were aligned to human genome build hg19 and sequence variants called with Isaac Genome Alignment

262 Software and variant caller ⁶⁵. Individual genomic variant call format files (GVCFs) were merged with
263 ‘agg’ tool: a utility for aggregating Illumina-style GVCFs. Following completion of the raw data merge,
264 multiple QC filtering steps were performed: (i) setting genotypes with GQ<10 to missing; (ii) removing
265 low-quality sites (QUAL< 30 and QUAL< 20 for SNPs and indels, respectively); (iii) removing sites with
266 missingness > 10%. (iv) Samples excluded if deviated from mean by more than 6SD for total numbers of
267 SNPs, singletons and indels, Ti/Tv ratio, het/hom-non-ref ratio and inbreeding (by cohort). (v) missingness
268 > 5%, (vi) genotyping-sequence concordance (made possible by genotyping data generated on the
269 Illumina Omni 2.5M SNP array for all samples; 96% concordance), (vii) depth of coverage, (viii) a gender
270 check (to identify mismatches), (ix) relatedness (drop samples with >100 relatedness pairs). (x) Related
271 individuals were further excluded until no pair of samples had a kinship coefficient > 0.05. (xi) missing
272 phenotype information. Following QC, 312 samples with expended/inconsistent *C9orf72* status were
273 omitted from further analysis. A total of 5,774 samples (3,955 ALS patients and 1,819 healthy controls)
274 passed all QC and were included in downstream analysis. Per-nucleotide site QC was performed on QC-
275 passing samples only, for Biallelic sites: variants were excluded from analysis based on depth (total DP <
276 10,000 or > 226,000), missingness > 5%, passing rate in the whole dataset < 70%, sites out of Hardy–
277 Weinberg equilibrium (HWE; by cohort, controls only, $p < 1 \times 10^{-6}$) and sites with extreme differential
278 missingness between cases and control samples (Overall and by cohort, $p < 1 \times 10^{-6}$). Non-autosomal
279 chromosomes and multiallelic variants were excluded from analysis.

280 **Selection of regions of interest**

281 Discontinuous regions of interest approximating in total ~5Mb, include coding sequences and 3’
282 untranslated regions (3’UTRs) of 295 genes ([Supplementary Table 3](#)) encoding for proteins that were: (i)
283 previously reported to be associated with ALS, (ii) RNA-binding proteins including miRNA biogenesis
284 or activity factors [UCSC gene annotation; ⁶⁶]. In addition to (iii) all 1,750 human pre-miRNA genes
285 [miRBase v20; ²⁹]. In addition, genome-wide analysis of all known human 3’UTRs (RefSeq ³⁶). Variants
286 in regions of interest were extracted from Project MinE ALS sequencing consortium genomes using
287 vcftools ⁶⁷ according to BED file containing genomic coordinates of interest (hg19) ± 300 bp that ensures
288 covering splice junctions and sequence ([Supplementary Table 7](#)).

289 **Annotation and burden analysis**

290 After quality control and extraction of regions of interest we performed functional annotation of all
291 variants. Indels were left-aligned and normalized using bcftools and multiallelic sites were removed. For
292 variant annotation we developed a pipeline that calculates the impact of genetic variation in coding regions
293 as well as in 3'UTR and miRNA regions, using ANNOVAR⁶⁸. The frequency of the variants in the general
294 population was assessed by screening the 1000 Genomes Project, the Exome Aggregation Consortium
295 (ExAC) and NHLBI Exome Sequencing Project (ESP). For protein coding ORFs, association analysis of
296 deleterious rare variants was performed, i.e., frameshift variants, deviation from canonical splice variant,
297 stop gain/loss variants or a non-synonymous substitution, as predicted by at least three prediction
298 programs (SIFT, Polyphen2 HVAR, LRT, MutationTaster, MutationAssessor, FATHMM, MetaLR) in
299 dbNSFP environment [v2.0;³⁰].

300 Non-coding sequence burden analysis included (i) 3'UTRs, (ii) variants in miRNA recognition elements
301 in 3'UTRs ([Supplementary Table 3](#)): Variants that impaired conserved-miRNA binding sites in 3'UTRs
302 (predicted loss of function) were called by TargetScan [v7.0;⁶⁹]. Newly created miRNA binding sites in
303 3'UTRs (predicted gain of function) were called by textual comparison of all possible mutated seeds
304 around a variant to all known miRNA seed sequences in the genome, (iii) all human pre-miRNAs (mirBase
305 v20²⁹) and (iv) miRNAs:target gene networks: mature miRNA sequences (mirBase v20²⁹) and cognate
306 targets within the 3'UTRs ([Supplementary Table 3](#)).

307 **Mammalian Cell Cultures**

308 Lymphoblastoid cell lines (LCLs) from the UK MNDA DNA Bank³⁸ were originally derived from an
309 individual carrying the suggested *IL18RAP* protective variant (V3, Chr2:103068718 G>A) and another
310 individual with the canonical *IL18RAP* 3'UTR (Weizmann IRB: 537-1). LCLs were cultured in RPMI-
311 1640 (Gibco, 21875091) with 20% inactivated fetal bovine serum (FBS, Biological Industries, 04-001-
312 1A), 1% L-glutamine and 1% penicillin-streptomycin (Biological Industries, 03-0311B) at 37°C, 5% CO₂.
313 Human Bone Osteosarcoma Epithelial Cells (U2OS), were maintained in Dulbecco's Modified Eagle
314 Medium (DMEM, Biological Industries, 01-050-1A) supplemented with 10% FBS, 1% penicillin-
315 streptomycin at 37°C, 5% CO₂.

316

317 **Cloning**

318 Full *IL18RAP* coding sequence (CDS) and 3'UTR sequence (2223bp) in pMX vector was purchased from
319 GeneArt (Invitrogen, [Supplementary Table 8](#)) and subcloned with V5 epitope into pcDNA3. Different
320 mutants, including: WT *IL18RAP* CDS + mutant 3'UTR (V1 or V3), and a dominant negative coding
321 mutant E210A-Y212A-Y214A CDS + WT 3'UTR (3CDS)³⁹ created by Transfer-PCR mutagenesis⁷⁰.
322 Next, WT and mutants full *IL18RAP* were subcloned into pUltra vector (a gift from Malcolm Moore,
323 Addgene plasmid #24130, for which mCherry was replaced with EGFP), downstream of the human
324 Ubiquitin C promoter and EGFP-P2A. Human *IL18RAP* 3'UTR sequences (422bp) in pMX vector were
325 purchased from GeneArt (Invitrogen, [Supplementary Table 8](#)) and subcloned into hRluc reporter in
326 psiCHECK-2 vector (Promega). All cloning procedures were done via restriction free cloning⁷¹. List of
327 primers used for cloning and Transfer-PCR mutagenesis described in [Supplementary Table 9](#).

328 **Transfection and luciferase assays**

329 Transfection to U2OS Cells at 1.9 cm² Corning plates was performed at 70–80% confluence, 24 h post
330 plating in antibiotic- free media, using Lipofectamine 2000, 0.5 μ L per well (Thermo Fisher Scientific,
331 Cat# 11668027). Each well was considered as a single replicate. miRNA sensor: U2OS cells were
332 harvested 72 h post-transfection with human *IL18RAP* 3'UTR downstream to hRluc reporter (psiCHECK-
333 2 vector 500 ng / 1.9 cm² plate), for Dual luciferase reporter assay (Promega). NF- κ B reporter assay:
334 U2OS cells were induced with recombinant IL-18 (5ng/ml) 72 h post-transfection with full coding
335 sequence of *IL18RAP* coding region + 3'UTRs (pUltra vector 500 ng / 1.9 cm² plate), luc2P/NF- κ B-RE
336 (pGL4.32 100 ng) luciferase and Renilla luciferase (hRluc 10 ng). 6 h post later cells were harvested and
337 luminescence quantified.

338 **Cell lysis and Western blot**

339 LCLs were washed in PBSx1, centrifuged at 800 \times g for 5 min at 4°C, pelleted and lysed in ice-cold RIPA
340 buffer supplemented with cComplete™ Protease Inhibitor Cocktail (Roche, 4693116001) and
341 PhosSTOP™ (Roche, 4906837001). The lysates were cleared by centrifugation at 15,000 \times g for 10 min
342 at 4°C. Plasma Membrane Protein Extraction Kit (abcam, ab65400) was used for extraction of membrane-
343 bound IL18RAP.

344 Protein concentrations quantified with Protein Assay Dye Reagent (Bio-Rad, 500-0006), resolved at 50 μ g
345 of total protein/well by 10% polyacrylamide / SDS gel electrophoresis at 100-120 V for 70 min. After gel
346 electrophoresis and transferred to nitrocellulose membrane (Whatmann, 10401383) at 250mA for 70 min.
347 Membranes were stained with Ponceau (Sigma, P7170), blocked for 1 hour at RT with 3% Bovine albumin
348 fraction V (MPBio 160069) or 5% milk protein in PBST (PBS containing 0.05% TWEEN-20) and then
349 incubated with primary antibodies [Rabbit anti IL-18R Beta antibody (Bioss, catalog# BS-2616R, 1:500),
350 mouse anti GAPDH (Thermo Fisher, catalog# AM4300, 1:5000), mouse anti p-NF κ B p65 antibody (Santa
351 Cruz, catalog# sc-135769, 1:200), Mouse Anti-beta Actin antibody [AC-15] (abcam, catalog# ab6276,
352 1:9,000)] O.N. at 4°C with rocking in antibody-Solution [5% albumin, 0.02% sodium azide, 5 drops of
353 phenol red in 0.05% PBST]. Following primary antibody incubation, membranes were washed 3 times for
354 5 min at RT with 0.05% PBST then incubated for 1 hour at RT with horseradish peroxidase (HRP)-
355 conjugated species-specific secondary antibodies, washed 3 x 5 min in 0.05% PBST at RT and visualized
356 using EZ-ECL Chemiluminescence (Biological Industries, 20500-120) by ImageQuant™ LAS 4000 (GE
357 Healthcare Life Sciences). Densitometric analysis performed using ImageJ (NIH).

358 **Induced neuron survival assay**

359 Survival assay of *Hb9::RFP+* iMNs was conducted as described previously⁴⁵, with the following
360 modifications: (i) iMNs were infected on day 2 with lentiviruses expressing the full pUltra-IL18RAP
361 constructs, and (ii) longitudinal microscopic tracking was performed every 48 hours, following
362 neurotrophic factor withdrawal and IL-18 treatment (10ng/mL), starting on day 15 for 18 additional days.
363 iMN survival assays were performed using three individual replicates / line / condition. iMNs were from
364 two independent donors for each genotype (CTRL/C9-ALS) were combined into one survival trace in the
365 Kaplan-Meier plots for clarity. Ichida lab human lymphocytes from healthy subjects and ALS patients
366 were obtained from the National Institute of Neurological Disorders and Stroke (NINDS) Biorepository
367 at the Coriell Institute for Medical Research and reprogrammed into iPSCs as previously described⁴⁵. The
368 NINDS Biorepository requires informed consent from patients. The experiment involved mouse glial
369 isolation, performed at University of Southern California (USC) and was done in compliance with ethical
370 regulations approved by the USC IACUC committee (Los Angeles, USA).

371 **Statistical analysis**

372 Statistics performed with Prism Origin (GraphPad). Shapiro-Wilk test was used to assess normality of the
373 data. Pairwise comparisons passing normality test were analyzed with Student's *t*-test, whereas the Mann-

374 Whitney test was used for pairwise comparison of nonparametric data. Multiple group comparisons were
375 analyzed using ANOVA with post hoc tests. For iMN survival experiments, statistical analysis was
376 performed using a one-sided log-rank test to account for events that did not occur (i.e. iMNs that did not
377 degenerate before the end of the experiment). For each line, the number of iMNs that were analyzed to
378 generate the survival curve is indicated in the figure. Statistical P values <0.05 were considered significant.
379 Data are shown as box plots, or as noted in the text.

380 **Supplementary Materials**

381 Fig. S1. Study design.

382 Fig. S2. Region-based rare-variant association analyses.

383 Fig. S3. 3'UTR-based rare-variant association analysis, using different algorithms.

384 Fig. S4. Evaluation of IL18RAP and IL-18 mRNA expression in motor neurons of patients with ALS.

385 Table S1. Total number of samples before and after quality control procedures, stratified by country.

386 Table S2. Samples Quality Control Procedures.

387 Table S3. Candidate genes list.

388 Table S4. Number of rare qualifying genetics variants identified.

389 Table S5. Identified *IL18RAP* 3'UTR variants in Project MinE discovery cohort.

390 Table S6. Identified *IL18RAP* 3'UTR variants in discovery and replication cohorts.

391 Table S7. BED file containing genomic coordinates of regions of interest.

392 Table S8. Synthetic *IL18RAP* sequences used for cloning into pMX vectors.

393 Table S9. List of primers used for cloning and Transfer-PCR mutagenesis.

394 Data File S1. Detailed description of variants in protein coding sequences of *NEK1* and *SOD1* and the
395 *IL18RAP* 3'UTR, in Project MinE discovery cohort.

396 Data File S2. Source data for IL18RAP western blot studies.

397 Data File S3. Source data for p-NF- κ B western blot studies.

398 Project MinE ALS Sequencing Consortium PI List

399 NYGC ALS Consortium PI List

400 **Acknowledgments:**

401 We gratefully acknowledge the contributions of all participants and the investigators who provided
402 biological samples and data for Project Mine ALS sequencing consortium, the New York Genome Center
403 (NYGC) ALS Consortium, the Genome Aggregation Database (gnomAD) and Trans-Omics for Precision
404 Medicine (TOPMed) of the National Heart, Lung, and Blood Institute (NHLBI,
405 <https://www.nhlbiwgs.org/topmed-banner-authorship>). Samples used in this research were in part
406 obtained from the UK National DNA Bank for MND Research, funded by the MND Association and the
407 Wellcome Trust. We acknowledge sample management undertaken by Biobanking Solutions funded by
408 the Medical Research Council at the Centre for Integrated Genomic Medical Research, University of
409 Manchester. The authors would like to thank the NINDS Biorepository at Coriell Institute for providing
410 the cell lines used for this study at J.K.I. lab. We thank LSE for language and scientific editing. Hornstein
411 lab is supported by friends of Dr. Sydney Brenner. EH is Head of Nella and Leon Benozio Center for
412 Neurological Diseases and incumbent of Ira & Gail Mondry Professorial chair. **Funding:** The work is
413 funded by Legacy Heritage Fund, Bruno and Ilse Frick Foundation for Research on ALS, Teva
414 Pharmaceutical Industries Ltd as part of the Israeli National Network of Excellence in Neuroscience
415 (NNE) and Minna-James-Heineman Stiftung through Minerva. The research leading to these results has
416 received funding to E.H. from the European Research Council under the European Union's Seventh
417 Framework Programme (FP7/2007-2013) / ERC grant agreement n° 617351. Israel Science Foundation,
418 the ALS-Therapy Alliance, AFM Telethon (20576 to E.H.), Motor Neuron Disease Association (UK),
419 The Thierry Latran Foundation for ALS research, ERA-Net for Research Programmes on Rare Diseases
420 (FP7), A. Alfred Taubman through IsrALS, Yeda-Sela, Yeda-CEO, Israel Ministry of Trade and Industry,
421 Y. Leon Benozio Institute for Molecular Medicine, Kekst Family Institute for Medical Genetics, David
422 and Fela Shapell Family Center for Genetic Disorders Research, Crown Human Genome Center, Nathan,
423 Shirley, Philip and Charlene Vener New Scientist Fund, Julius and Ray Charlestein Foundation, Fraida
424 Foundation, Wolfson Family Charitable Trust, Adelis Foundation, MERCK (UK), Maria Halphen, Estates
425 of Fannie Sherr, Lola Asseof, Lilly Fulop. To A.A.C. from Neurodegenerative Disease Research (JPND),
426 Medical Research Council (MR/L501529/1; STRENGTH, MR/R024804/1; BRAIN-MEND), Economic
427 and Social Research Council (ES/L008238/1; ALS-CarE), MND Association. National Institute for
428 Health Research (NIHR) Biomedical Research Centre at South London and Maudsley NHS Foundation
429 Trust and King's College London. To P.V.D.: Project MinE Belgium was supported by a grant from IWT
430 (n° 140935), the ALS Liga België, the National Lottery of Belgium and the KU Leuven Opening the

431 Future Fund. P.V.D. holds a senior clinical investigatorship of FWO-Vlaanderen and is supported by E.
432 von Behring Chair for Neuromuscular and Neurodegenerative Disorders, the ALS Liga België and the
433 KU Leuven funds “Een Hart voor ALS”, “Laeversfonds voor ALS Onderzoek” and the “Valéry Perrier
434 Race against ALS Fund”. Several authors of this publication are members of the European Reference
435 Network for Rare Neuromuscular Diseases (ERN-NMD). To P.J.S.: from the Medical Research Council,
436 MND Association, NIHR Senior Investigator Award, National Institute for Health Research (NIHR)
437 Sheffield Biomedical Research Centre and NIHR Sheffield Clinical Research Facility. To P.M.A.: Knut
438 and Alice Wallenberg Foundation, the Swedish Brain Foundation, the Swedish Science Council, the Ulla-
439 Carin Lindquist Foundation. H.P.P. and sequencing activities at NYGC were supported by the ALS
440 Association (ALSA) and The Tow Foundation. C.E. was supported by scholarship from Teva
441 Pharmaceutical Industries Ltd as part of the Israeli National Network of Excellence in Neuroscience
442 (NNE). S.M.K.F. is supported by the ALS Canada Tim E. Noël Postdoctoral Fellowship. R. H. Brown Jr.
443 was funded by ALS Association, ALS Finding a Cure, Angel Fund, ALS-One, Cellucci Fund and NIH
444 grants (R01 NS104022, R01 NS073873 and NS111990-01 to R.H.B.J.). J.K.I. is a New York Stem Cell
445 Foundation-Robertson Investigator. Work at J.K.I. lab was supported by NIH grants R01NS097850, U.S.
446 Department of Defense grant W81XWH-19-PRARP-CSRA, and grants from the Tau Consortium, the
447 New York Stem Cell Foundation, the ALS Association, and the John Douglas French Alzheimer’s
448 Foundation. To R.L.McL.: Science Foundation Ireland (17/CDA/4737). To A.N.B.: Suna and Inan Kirac
449 Foundation. To J.E.L.: National Institute of Health/NINDS (R01 NS073873). **Author contributions:** C.E.
450 led the project; C.E. contributed to research conception, design and interpretations and wrote the
451 manuscript with E.H.; C.E., E.B., T.O., K.R.V.E., S.L.P., M.M., S.M.K.F., N.Y., J.C.-K., K.P.K.,
452 R.A.A.V.D.S., W.S., A.A.K., A.I., A.S., A.R.J., E.C., D.R., O.W., R.H.B.J., P.J.S., P.V.D., L.H.V.D.B.,
453 H.P.P., E.S., A.A.-C. and J.H.V. collected samples, were involved in the sequence analysis pipeline,
454 phenotyping, variant calling, provided expertise or were involved in the genetic association analysis of
455 rare non-coding variants in human patients with ALS; S.-T.H. and J.K.I. performed iMNs experiments
456 and interpreted data; A.S. and C.E. performed molecular biology studies in LCLs and U2OS cell lines,
457 including reporter assays and protein quantification by western blots; S.W. and D.P.S. helped performing
458 research; E.H. conceived and supervised the study and wrote the manuscript with C.E. All co-authors
459 provided approval of the manuscript. **Competing interests:** J.K.I. is a co-founder of AcuraStem
460 Incorporated. J.K.I. declares that he is bound by confidentiality agreements that prevent him from
461 disclosing details of his financial interests in this work. E.H. is inventor on pending patent family

462 PCT/IL2016/050328 entitled “Methods of treating motor neuron diseases”. All other authors declare that
463 they have no competing interests. **Data availability:** Human genetics data is publically available from the
464 sequencing consortia: Project Mine ALS sequencing consortium, the New York Genome Center (NYGC)
465 ALS Consortium, the Genome Aggregation Database (gnomAD) and NHLBI's Trans-Omics for Precision
466 Medicine (TOPMed). All Other data used for this manuscript are available in the manuscript. **Code**
467 **availability:** Variant annotation scripts are available at GitHub: [https://github.com/TsviyaOlender/Non-](https://github.com/TsviyaOlender/Non-coding-Variants-in-ALS-genes-)
468 [coding-Variants-in-ALS-genes-](https://github.com/TsviyaOlender/Non-coding-Variants-in-ALS-genes-).

469 **References**

470

- 471 1. Cookson, W., Liang, L., Abecasis, G., Moffatt, M. & Lathrop, M. Mapping complex disease
472 traits with global gene expression. *Nature reviews. Genetics* **10**, 184-194 (2009).
- 473 2. Knight, J.C. Regulatory polymorphisms underlying complex disease traits. *Journal of molecular*
474 *medicine* **83**, 97-109 (2005).
- 475 3. Brown, R.H. & Al-Chalabi, A. Amyotrophic Lateral Sclerosis. *The New England journal of*
476 *medicine* **377**, 162-172 (2017).
- 477 4. Taylor, J.P., Brown, R.H., Jr. & Cleveland, D.W. Decoding ALS: from genes to mechanism.
478 *Nature* **539**, 197-206 (2016).
- 479 5. Renton, A.E., Chio, A. & Traynor, B.J. State of play in amyotrophic lateral sclerosis genetics.
480 *Nature neuroscience* **17**, 17-23 (2014).
- 481 6. Al-Chalabi, A., van den Berg, L.H. & Veldink, J. Gene discovery in amyotrophic lateral
482 sclerosis: implications for clinical management. *Nat Rev Neurol* **13**, 96-104 (2017).
- 483 7. DeJesus-Hernandez, M., *et al.* Expanded GGGGCC hexanucleotide repeat in noncoding region
484 of C9ORF72 causes chromosome 9p-linked FTD and ALS. *Neuron* **72**, 245-256 (2011).
- 485 8. Renton, A.E., *et al.* A hexanucleotide repeat expansion in C9ORF72 is the cause of chromosome
486 9p21-linked ALS-FTD. *Neuron* **72**, 257-268 (2011).
- 487 9. La Spada, A.R. & Taylor, J.P. Repeat expansion disease: progress and puzzles in disease
488 pathogenesis. *Nature reviews. Genetics* **11**, 247-258 (2010).
- 489 10. Haramati, S., *et al.* miRNA malfunction causes spinal motor neuron disease. *Proceedings of the*
490 *National Academy of Sciences of the United States of America* **107**, 13111-13116 (2010).
- 491 11. Emde, A., *et al.* Dysregulated miRNA biogenesis downstream of cellular stress and ALS-causing
492 mutations: a new mechanism for ALS. *The EMBO journal* **34**, 2633-2651 (2015).
- 493 12. Eitan, C. & Hornstein, E. Vulnerability of microRNA biogenesis in FTD-ALS. *Brain research*
494 (2016).
- 495 13. Campos-Melo, D., Droppelmann, C.A., He, Z., Volkening, K. & Strong, M.J. Altered microRNA
496 expression profile in Amyotrophic Lateral Sclerosis: a role in the regulation of NFL mRNA levels.
497 *Molecular brain* **6**, 26 (2013).
- 498 14. Buratti, E., *et al.* Nuclear factor TDP-43 can affect selected microRNA levels. *The FEBS journal*
499 **277**, 2268-2281 (2010).

- 500 15. Kawahara, Y. & Mieda-Sato, A. TDP-43 promotes microRNA biogenesis as a component of the
501 Drosha and Dicer complexes. *Proceedings of the National Academy of Sciences of the United States of*
502 *America* **109**, 3347-3352 (2012).
- 503 16. Morlando, M., *et al.* FUS stimulates microRNA biogenesis by facilitating co-transcriptional
504 Drosha recruitment. *The EMBO journal* **31**, 4502-4510 (2012).
- 505 17. Hoye, M.L., *et al.* MicroRNA Profiling Reveals Marker of Motor Neuron Disease in ALS
506 Models. *J Neurosci* **37**, 5574-5586 (2017).
- 507 18. Rotem, N., *et al.* ALS Along the Axons - Expression of Coding and Noncoding RNA Differs in
508 Axons of ALS models. *Sci Rep* **7**, 44500 (2017).
- 509 19. Butovsky, O., *et al.* Modulating inflammatory monocytes with a unique microRNA gene
510 signature ameliorates murine ALS. *J Clin Invest* **122**, 3063-3087 (2012).
- 511 20. Figueroa-Romero, C., *et al.* Expression of microRNAs in human post-mortem amyotrophic
512 lateral sclerosis spinal cords provides insight into disease mechanisms. *Mol Cell Neurosci* **71**, 34-45
513 (2016).
- 514 21. Williams, A.H., *et al.* MicroRNA-206 delays ALS progression and promotes regeneration of
515 neuromuscular synapses in mice. *Science* **326**, 1549-1554 (2009).
- 516 22. Bartel, D.P. MicroRNAs: target recognition and regulatory functions. *Cell* **136**, 215-233 (2009).
- 517 23. Mayr, C. Regulation by 3'-Untranslated Regions. *Annual review of genetics* **51**, 171-194 (2017).
- 518 24. Povysil, G., *et al.* Rare-variant collapsing analyses for complex traits: guidelines and
519 applications. *Nature reviews. Genetics* **20**, 747-759 (2019).
- 520 25. An, J.Y., *et al.* Genome-wide de novo risk score implicates promoter variation in autism
521 spectrum disorder. *Science* **362** (2018).
- 522 26. Lee, S., Abecasis, G.R., Boehnke, M. & Lin, X. Rare-variant association analysis: study designs
523 and statistical tests. *American journal of human genetics* **95**, 5-23 (2014).
- 524 27. Project MinE Consortium, Van Rheenen, W. & *et al.* Project MinE: study design and pilot
525 analyses of a large-scale whole-genome sequencing study in amyotrophic lateral sclerosis. (2017).
- 526 28. Dunckley, T., *et al.* Whole-genome analysis of sporadic amyotrophic lateral sclerosis. *The New*
527 *England journal of medicine* **357**, 775-788 (2007).
- 528 29. Griffiths-Jones, S., Grocock, R.J., van Dongen, S., Bateman, A. & Enright, A.J. miRBase:
529 microRNA sequences, targets and gene nomenclature. *Nucleic acids research* **34**, D140-144 (2006).

- 530 30. Liu, X., Jian, X. & Boerwinkle, E. dbNSFP v2.0: a database of human non-synonymous SNVs
531 and their functional predictions and annotations. *Human mutation* **34**, E2393-2402 (2013).
- 532 31. Lee, S., *et al.* Optimal unified approach for rare-variant association testing with application to
533 small-sample case-control whole-exome sequencing studies. *American journal of human genetics* **91**,
534 224-237 (2012).
- 535 32. Kenna, K.P., *et al.* NEK1 variants confer susceptibility to amyotrophic lateral sclerosis. *Nature*
536 *genetics* **48**, 1037-1042 (2016).
- 537 33. Rosen, D.R., *et al.* Mutations in Cu/Zn superoxide dismutase gene are associated with familial
538 amyotrophic lateral sclerosis. *Nature* **362**, 59-62 (1993).
- 539 34. Chio, A., *et al.* Prevalence of SOD1 mutations in the Italian ALS population. *Neurology* **70**, 533-
540 537 (2008).
- 541 35. van der Spek, R.A.A., *et al.* The project MinE databrowser: bringing large-scale whole-genome
542 sequencing in ALS to researchers and the public. *Amyotrophic lateral sclerosis & frontotemporal*
543 *degeneration* **20**, 432-440 (2019).
- 544 36. O'Leary, N.A., *et al.* Reference sequence (RefSeq) database at NCBI: current status, taxonomic
545 expansion, and functional annotation. *Nucleic acids research* **44**, D733-745 (2016).
- 546 37. Alboni, S., Cervia, D., Sugama, S. & Conti, B. Interleukin 18 in the CNS. *Journal of*
547 *neuroinflammation* **7**, 9 (2010).
- 548 38. Smith, L., *et al.* Establishing the UK DNA Bank for motor neuron disease (MND). *BMC Genet*
549 **16**, 84-84 (2015).
- 550 39. Tsutsumi, N., *et al.* The structural basis for receptor recognition of human interleukin-18. *Nature*
551 *communications* **5**, 1-13 (2014).
- 552 40. Kadhim, H., Deltenre, P., Martin, J.J. & Sebire, G. In-situ expression of Interleukin-18 and
553 associated mediators in the human brain of sALS patients: Hypothesis for a role for immune-
554 inflammatory mechanisms. *Medical hypotheses* **86**, 14-17 (2016).
- 555 41. Johann, S., *et al.* NLRP3 inflammasome is expressed by astrocytes in the SOD1 mouse model of
556 ALS and in human sporadic ALS patients. *Glia* **63**, 2260-2273 (2015).
- 557 42. Italiani, P., *et al.* Evaluating the levels of interleukin-1 family cytokines in sporadic amyotrophic
558 lateral sclerosis. *Journal of neuroinflammation* **11**, 94 (2014).
- 559 43. Krach, F., *et al.* Transcriptome–pathology correlation identifies interplay between TDP-43 and
560 the expression of its kinase CK1E in sporadic ALS. *Acta neuropathologica* **136**, 405-423 (2018).

- 561 44. Thompson, L. iMN (Exp 2)—ALS. *SMA and control (unaffected) iMN cell lines differentiated*
562 *from iPS cell lines using a long differentiation protocol—RNA-seq., LINCS (collection)* (2017).
- 563 45. Shi, Y., *et al.* Haploinsufficiency leads to neurodegeneration in C9ORF72 ALS/FTD human
564 induced motor neurons. *Nature medicine* **24**, 313 (2018).
- 565 46. Ayers, K.L., *et al.* A loss of function variant in CASP7 protects against Alzheimer's disease in
566 homozygous APOE epsilon4 allele carriers. *BMC genomics* **17 Suppl 2**, 445 (2016).
- 567 47. Benitez, B.A., *et al.* Missense variant in TREML2 protects against Alzheimer's disease.
568 *Neurobiology of aging* **35**, 1510 e1519-1526 (2014).
- 569 48. Jonsson, T., *et al.* A mutation in APP protects against Alzheimer's disease and age-related
570 cognitive decline. *Nature* **488**, 96-99 (2012).
- 571 49. Sims, R., *et al.* Rare coding variants in PLCG2, ABI3, and TREM2 implicate microglial-
572 mediated innate immunity in Alzheimer's disease. *Nature genetics* (2017).
- 573 50. Landers, J.E., *et al.* Reduced expression of the Kinesin-Associated Protein 3 (KIFAP3) gene
574 increases survival in sporadic amyotrophic lateral sclerosis. *Proceedings of the National Academy of*
575 *Sciences of the United States of America* **106**, 9004-9009 (2009).
- 576 51. Farhan, S.M.K., *et al.* Exome sequencing in amyotrophic lateral sclerosis implicates a novel
577 gene, DNAJC7, encoding a heat-shock protein. *Nature neuroscience* **22**, 1966-1974 (2019).
- 578 52. Lambrechts, D., *et al.* VEGF is a modifier of amyotrophic lateral sclerosis in mice and humans
579 and protects motoneurons against ischemic death. *Nature genetics* **34**, 383-394 (2003).
- 580 53. Beers, D.R. & Appel, S.H. Immune dysregulation in amyotrophic lateral sclerosis: Mechanisms
581 and emerging therapies. *The Lancet Neurology* **18**, 211-220 (2019).
- 582 54. Engelhardt, J.I. & Appel, S.H. IgG reactivity in the spinal cord and motor cortex in amyotrophic
583 lateral sclerosis. *Archives of neurology* **47**, 1210-1216 (1990).
- 584 55. Engelhardt, J.I., Tajti, J. & Appel, S.H. Lymphocytic infiltrates in the spinal cord in amyotrophic
585 lateral sclerosis. *Archives of neurology* **50**, 30-36 (1993).
- 586 56. Henkel, J.S., *et al.* Presence of dendritic cells, MCP-1, and activated microglia/macrophages in
587 amyotrophic lateral sclerosis spinal cord tissue. *Annals of neurology* **55**, 221-235 (2004).
- 588 57. Philips, T. & Robberecht, W. Neuroinflammation in amyotrophic lateral sclerosis: role of glial
589 activation in motor neuron disease. *The Lancet. Neurology* **10**, 253-263 (2011).

- 590 58. Zhernakova, A., *et al.* Genetic analysis of innate immunity in Crohn's disease and ulcerative
591 colitis identifies two susceptibility loci harboring CARD9 and IL18RAP. *American journal of human*
592 *genetics* **82**, 1202-1210 (2008).
- 593 59. Hirota, T., *et al.* Genome-wide association study identifies eight new susceptibility loci for
594 atopic dermatitis in the Japanese population. *Nature genetics* **44**, 1222-1226 (2012).
- 595 60. Liu, H., *et al.* Identification of IL18RAP/IL18R1 and IL12B as leprosy risk genes demonstrates
596 shared pathogenesis between inflammation and infectious diseases. *American journal of human genetics*
597 **91**, 935-941 (2012).
- 598 61. Hunt, K.A., *et al.* Newly identified genetic risk variants for celiac disease related to the immune
599 response. *Nature genetics* **40**, 395-402 (2008).
- 600 62. Smyth, D.J., *et al.* Shared and distinct genetic variants in type 1 diabetes and celiac disease. *The*
601 *New England journal of medicine* **359**, 2767-2777 (2008).
- 602 63. Leal-Lasarte, M.M., Franco, J.M., Labrador-Garrido, A., Pozo, D. & Roodveldt, C. Extracellular
603 TDP-43 aggregates target MAPK/MAK/MRK overlapping kinase (MOK) and trigger caspase-3/IL-18
604 signaling in microglia. *FASEB journal : official publication of the Federation of American Societies for*
605 *Experimental Biology* **31**, 2797-2816 (2017).
- 606 64. Zhan, X., Hu, Y., Li, B., Abecasis, G.R. & Liu, D.J. RVTESTS: an efficient and comprehensive
607 tool for rare variant association analysis using sequence data. *Bioinformatics* **32**, 1423-1426 (2016).
- 608 65. Raczy, C., *et al.* Isaac: ultra-fast whole-genome secondary analysis on Illumina sequencing
609 platforms. *Bioinformatics* **29**, 2041-2043 (2013).
- 610 66. Tyner, C., *et al.* The UCSC Genome Browser database: 2017 update. *Nucleic acids research* **45**,
611 D626-D634 (2017).
- 612 67. Danecek, P., *et al.* The variant call format and VCFtools. *Bioinformatics* **27**, 2156-2158 (2011).
- 613 68. Wang, K., Li, M. & Hakonarson, H. ANNOVAR: functional annotation of genetic variants from
614 high-throughput sequencing data. *Nucleic acids research* **38**, e164 (2010).
- 615 69. Agarwal, V., Bell, G.W., Nam, J.W. & Bartel, D.P. Predicting effective microRNA target sites in
616 mammalian mRNAs. *eLife* **4** (2015).
- 617 70. Erijman, A., Dantes, A., Bernheim, R., Shifman, J.M. & Peleg, Y. Transfer-PCR (TPCR): a
618 highway for DNA cloning and protein engineering. *Journal of structural biology* **175**, 171-177 (2011).
- 619 71. Peleg, Y. & Unger, T. Application of the Restriction-Free (RF) cloning for multicomponents
620 assembly. *Methods in molecular biology* **1116**, 73-87 (2014).

621 **FIGURES**

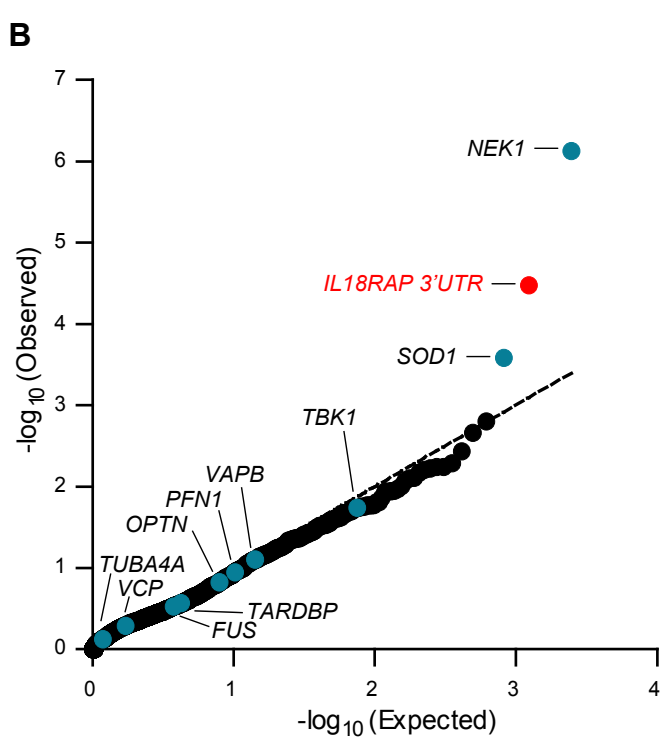
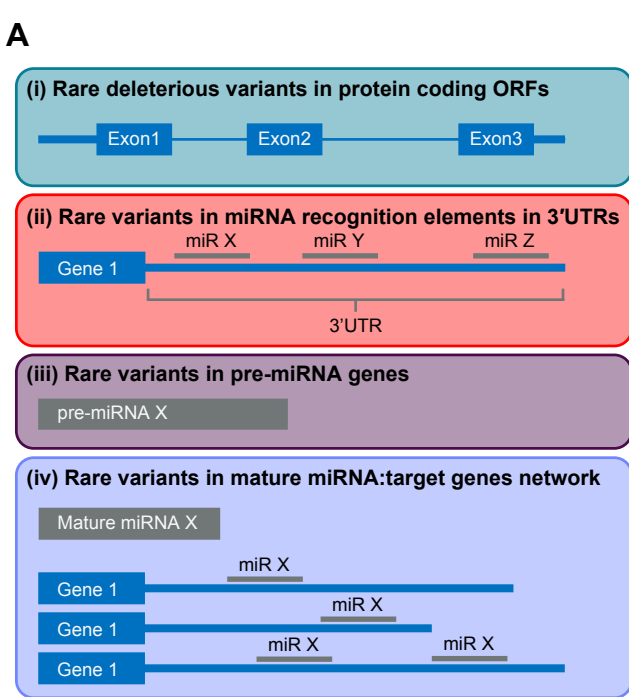


Fig.1 - Eitan et al. (Hornstein)

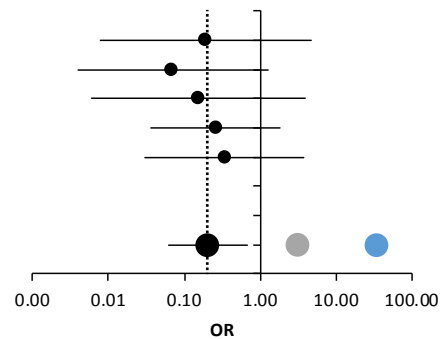
622 **Fig. 1. Region-based rare-variant association analysis.** (A) Diagram for region-based rare-variant
623 association studies. Collapsed region-based association analysis was performed on rare ($MAF \leq 0.01$)
624 qualifying variants in: (i) 295 candidate protein-coding genes (Supplementary Table 3) encoding for ALS-
625 relevant proteins or proteins associated with miRNA biogenesis/activity. Variants were included if
626 predicted to cause frameshifting, alternative splicing, an abnormal stop codon, or a deleterious non-
627 synonymous amino acid substitution, in ≥ 3 of 7 independent dbNSFP prediction algorithms; (ii) variants
628 abrogating or gaining miRNA recognition elements in 3'UTRs of the 295 genes (Supplementary Table 3);
629 (iii) all known pre-miRNA genes in the human genome; and (iv) predicted networks, comprised of
630 aggregated variants detected in a specific mature miRNA sequence and its cognate down-stream 3'UTR
631 targets. (B) QQ plot of obtained and expected P-values for the burden of rare variants (log scale) gained
632 by collapsed region-based association analysis of all genomic regions described in (A). Data were obtained
633 from 3,955 ALS cases and 1,819 controls (Project MinE). Features positioned on the diagonal line
634 represent results obtained under the null hypothesis. Open-reading frames of 10 known ALS genes (blue).
635 *IL18RAP* 3'UTR miRNA recognition elements (red). Genomic inflation $\lambda = 1.21$.

A

| Gene | Region | ALS (3955) | Control (1819) | OR | OR 95% CI | P | P corrected |
|---------|-------------------------------|------------|----------------|-------|-------------|-----------------------|-----------------------|
| NEK1 | Coding | 127 | 19 | 3.14 | 1.93-5.11 | 7.04x10 ⁻⁷ | 2.13x10 ⁻⁴ |
| SOD1 | Coding | 36 | 0 | 33.89 | 2.08-552.47 | 2.61x10 ⁻⁴ | 3.76x10 ⁻² |
| IL18RAP | miRNA bindings sites in 3'UTR | 4 | 9 | 0.20 | 0.06-0.66 | 3.34x10 ⁻⁵ | 9.31x10 ⁻³ |
| IL18RAP | 3'UTR | 6 | 12 | 0.23 | 0.09-0.61 | 1.88x10 ⁻⁵ | 5.62x10 ⁻³ |

B

| Cohort | Cases | Control | OR | OR 95% CI |
|---------------|--------|---------|------|-------------|
| Ireland | 0/239 | 1/136 | 0.19 | 0.008-4.662 |
| Netherlands | 0/1633 | 4/1004 | 0.07 | 0.004-1.265 |
| Turkey | 0/142 | 1/67 | 0.16 | 0.006-3.870 |
| UnitedKingdom | 2/1043 | 2/272 | 0.26 | 0.036-1.850 |
| USA | 2/398 | 1/68 | 0.34 | 0.030-3.784 |
| Belgium | 0/295 | 0/172 | - | - |
| Spain | 0/205 | 0/100 | - | - |
| Total | 4/3955 | 9/1819 | 0.20 | 0.063-0.662 |



C

| Cohort | Cases | Control | OR | 95% CI | P | |
|---|---------|-----------|------|-------------|-------------------------|-----------------------|
| | | | | | χ ² | SKAT-O |
| Discovery: Project MinE | 6/3955 | 12/1819 | 0.23 | 0.086-0.611 | 3.00x10 ⁻³ | 1.88x10 ⁻⁵ |
| Replication: NYGC, TOPMed & gnomAD | 8/2184 | 786/68584 | 0.32 | 0.158-0.637 | 9.58 x10 ⁻⁴ | - |
| Joint analysis: Discovery & replication | 14/6139 | 798/70403 | 0.20 | 0.118-0.338 | < 1.00x10 ⁻⁵ | - |

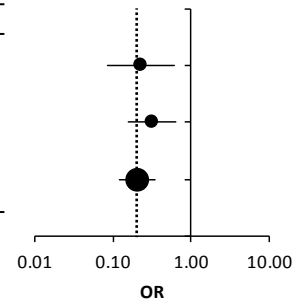


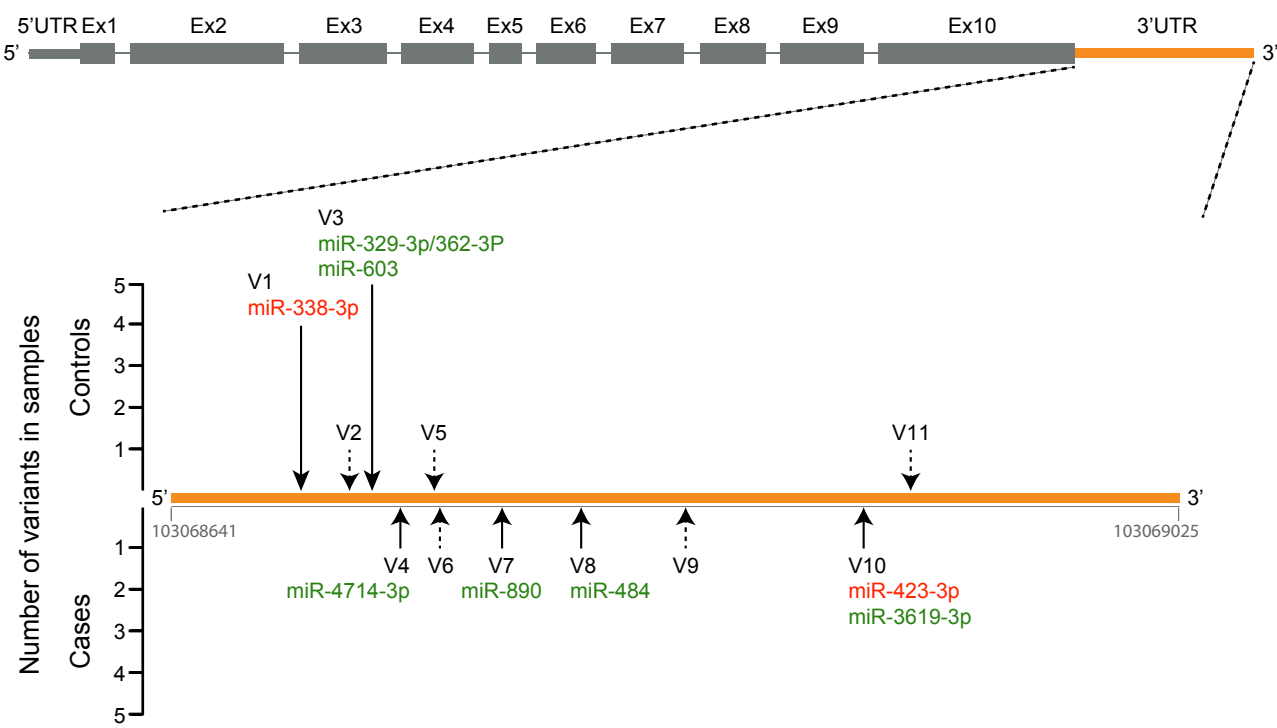
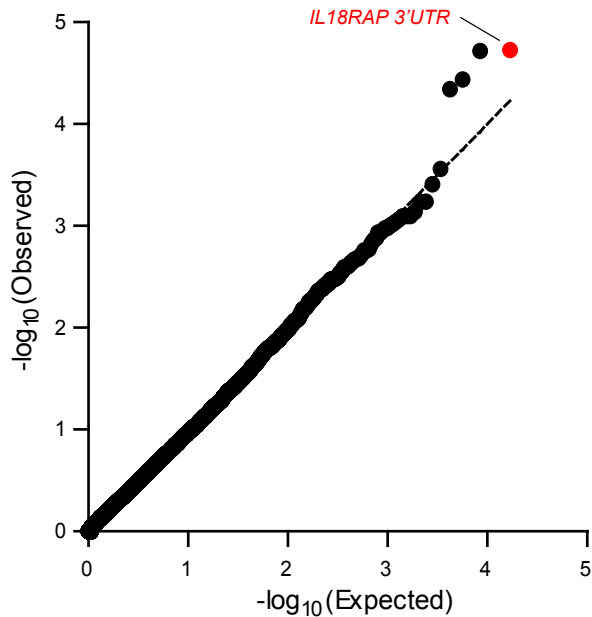
Fig.2 - Eitan et al. (Hornstein)

636 **Fig 2. Odds of ALS is reduced with rare variants in the *IL18RAP* 3'UTR.** (A) Odds ratio (OR)
637 estimates with 95% confidence intervals (CI) for *NEK1* (coding), *SOD1* (coding), predicted miRNA
638 recognition elements in the *IL18RAP* 3'UTR, and for all variants identified in the *IL18RAP* 3'UTR. P
639 values corrected for false discovery rate (FDR). (B) Stratification of data pertaining to miRNA recognition
640 elements in the *IL18RAP* 3'UTR in seven geographically-based sALS sub-cohorts and forest plot (Log
641 scale). *NEK1* (grey) and *SOD1* (blue) signals are from combined data of all cohorts. Vertical dotted line
642 denotes OR=0.2. (C) OR with 95% CI and forest plot (Log scale) across discovery and replication cohorts
643 and joint analysis thereof. Vertical dotted line denotes OR=0.2. P-values, calculated with SKAT-O or Chi-
644 squared test with Yate's correction.

A**Human IL18RAP**

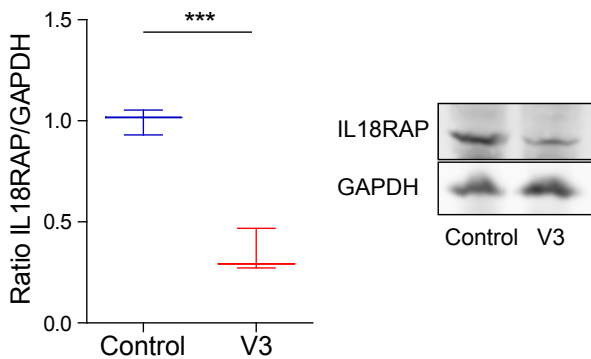
ENST00000264260 Chr2:103035149-103069025 [GRCh37/hg19]

3'UTR length: 384 Chr2:103068641-103069025 [GRCh37/hg19]

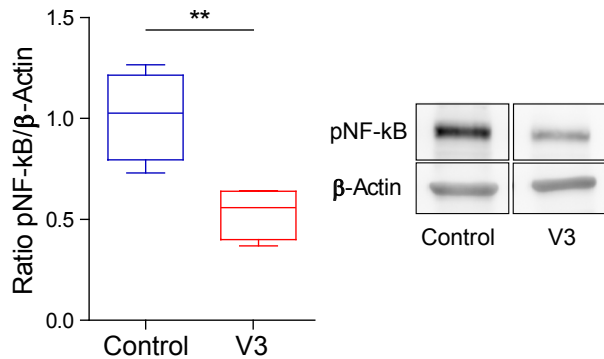
**B**

645 **Fig. 3. Rare variants in the *IL18RAP* 3'UTR.** (A) Schematic of the *IL18RAP* transcript and 3'UTR (5'
646 to 3') showing the number of control (upper) or ALS (lower) samples, in which miRNA recognition
647 element variants (black arrow) or other variants (dashed arrow) were identified. Potentially lost (red) or
648 created (green) miRNA recognition elements are marked (Supplementary Table 6). (B) QQ plot of
649 obtained and expected P-values for the burden of rare variants (log scale) gained by collapsed region-
650 based association analysis for all known human 3'UTRs (RefSeq), in Project MinE cohort (3,955 ALS
651 cases and 1,819 non-ALS controls). Variants are not restricted to miRNA recognition elements. Features
652 positioned on the diagonal line represent results obtained under the null hypothesis. The *IL18RAP* 3'UTR
653 (red) is the most significant 3'UTR associated with ALS. Genomic inflation $\lambda = 0.97$.

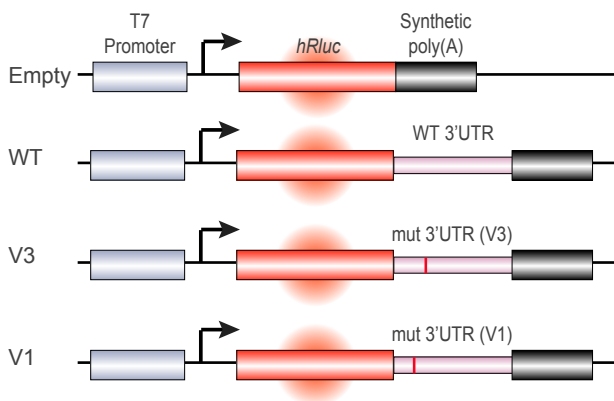
A Lymphoblastoid cell lines



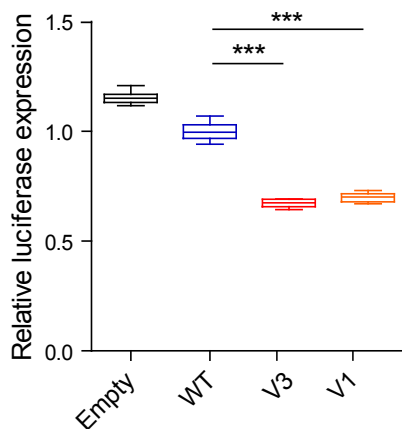
B



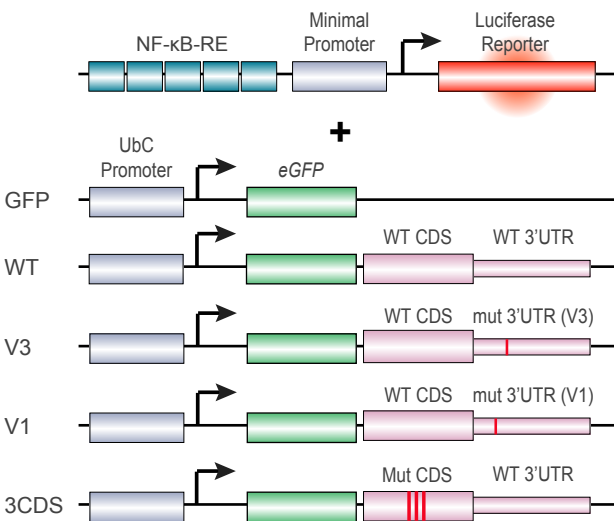
C Biosensor for 3'UTR variant activity



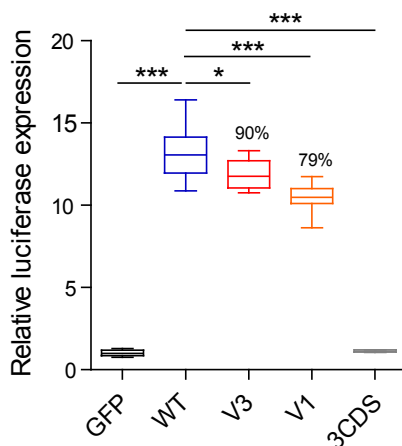
D U2OS cells



E Biosensor for NF-kB pathway activity

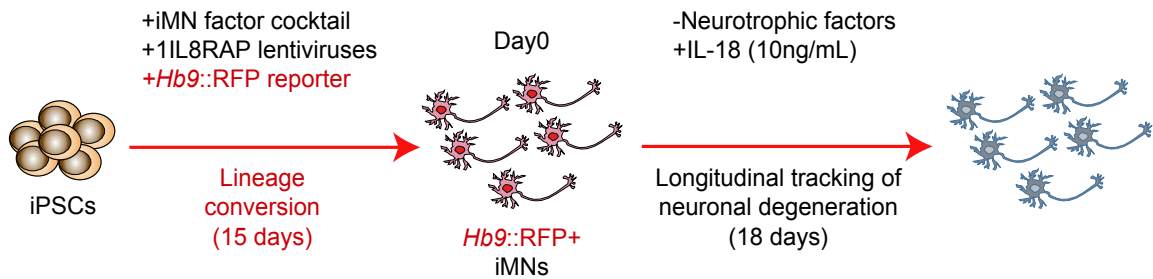


F U2OS cells

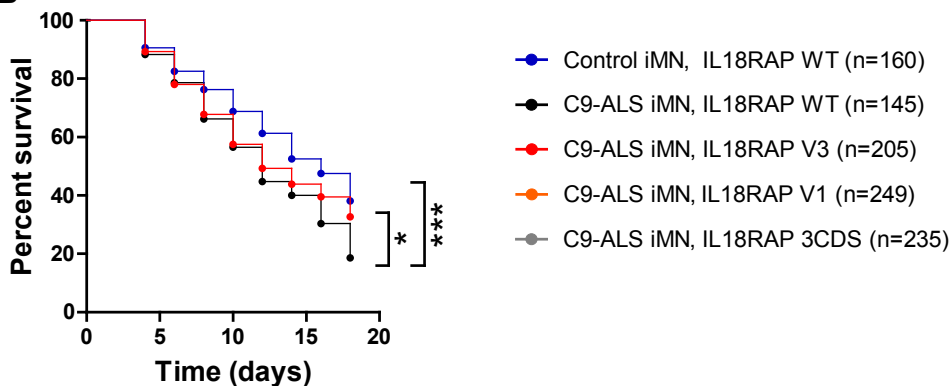


654 **Fig 4. *IL18RAP* 3'UTR variant attenuates IL-18 / NF- κ B signaling.** Quantification of protein
655 expression for IL18RAP (n=3) (**A**) or p-NF- κ B protein (n=4) (**B**) by Western blots of extracts from a
656 lymphoblastoid cell line harboring an endogenous IL18RAP variant (V3, Chr2:103068718 G>A) relative
657 to IL18RAP protein in a line with the canonical *IL18RAP* 3'UTR. Loading normalization with anti
658 GAPDH or anti Beta-Actin. Two-sided student *t*-test. Diagram (**C**) and quantification (**D**) of hRluc
659 *IL18RAP* 3'UTR reporter assays, in human U2OS cell line (Empty, WT, V3, V1; n=6). One-way ANOVA
660 followed by Dunnett's multiple comparison test. Diagram (**E**) and quantification (**F**) of NF- κ B reporter
661 assay in human U2OS cell line (GFP, WT, V3, V1, n=9; 3CDS, n=4). One-way ANOVA followed by
662 Dunnett's multiple comparison test was performed on square root-transformed data. Box plots depicting
663 median, upper and lower quartiles, and extreme points. * P<0.05; ** P<0.01; *** P<0.001. Experiment
664 repeated independently three times with similar results.

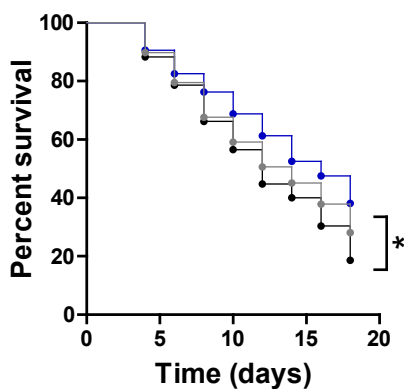
A C9ORF72 patients iMNs



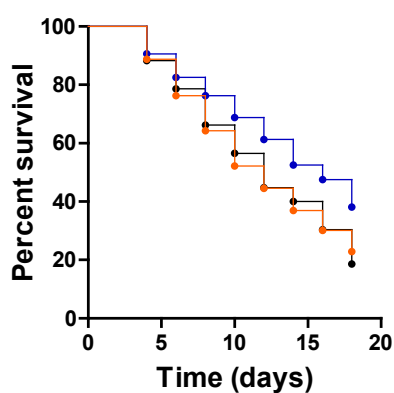
B



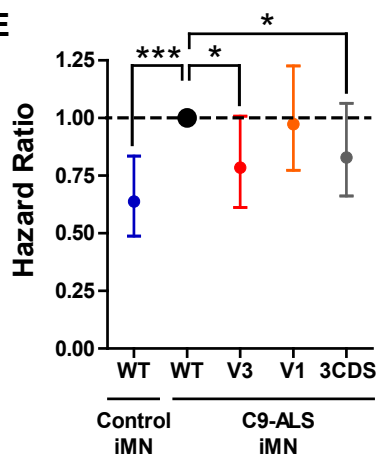
C



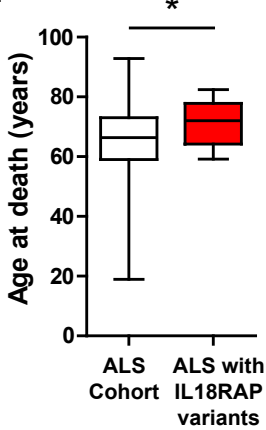
D



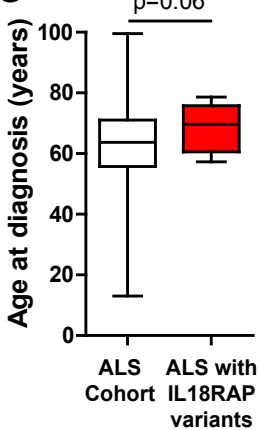
E



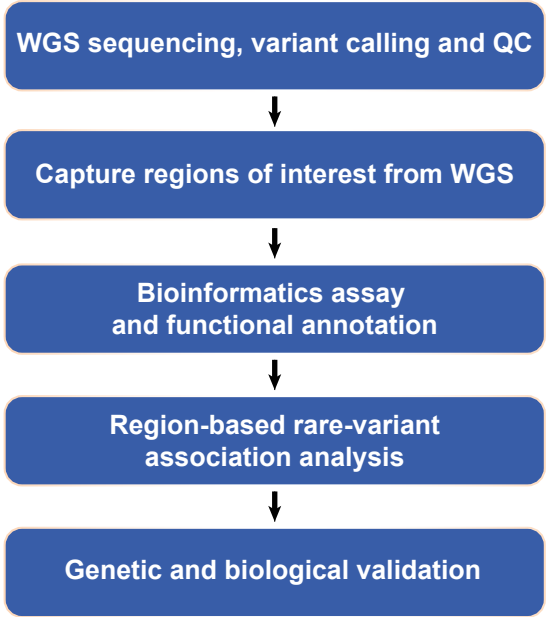
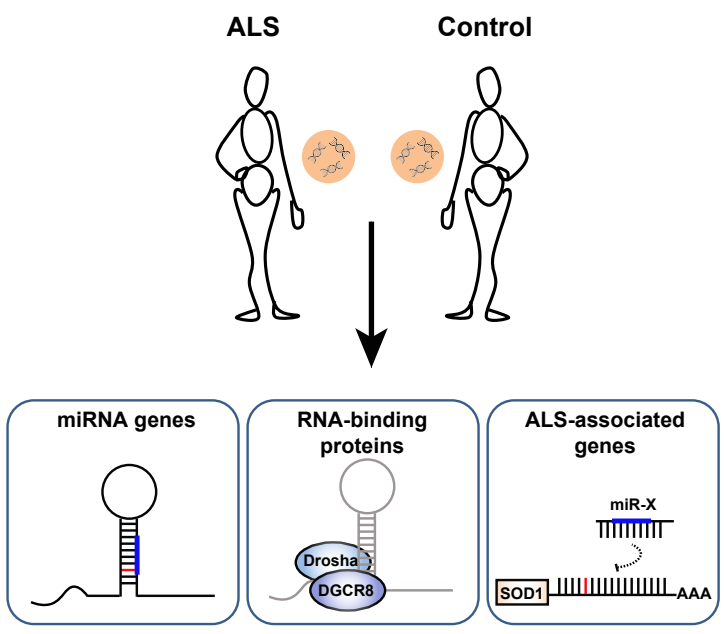
F



G

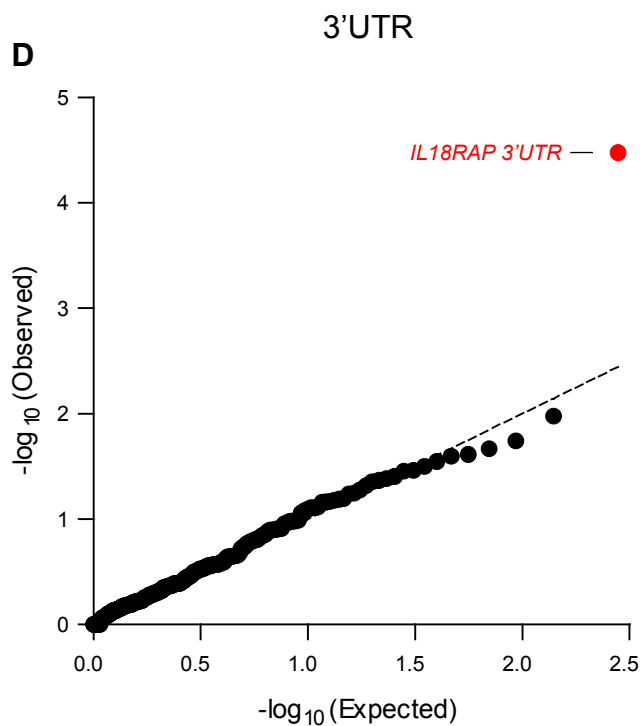
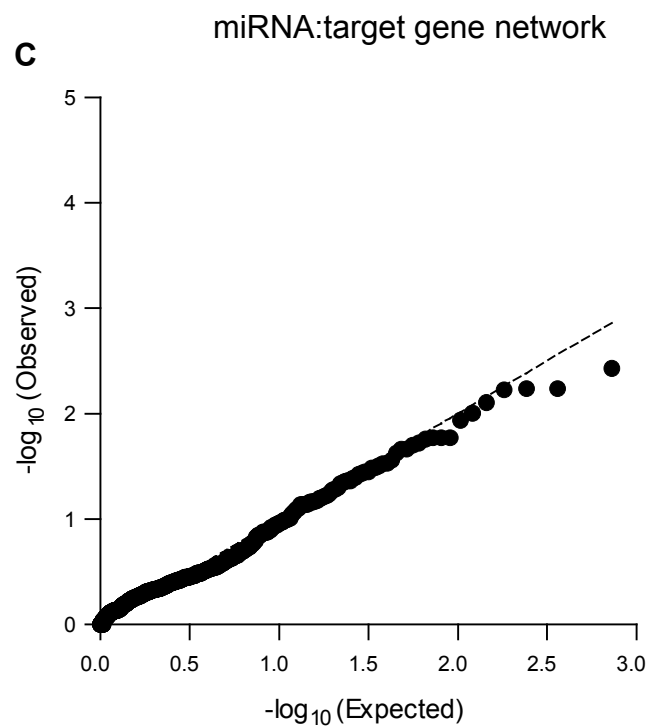
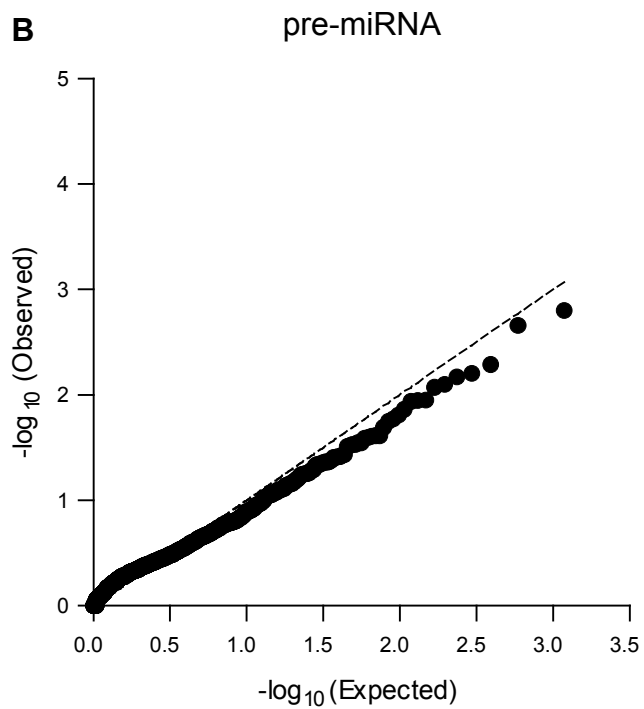
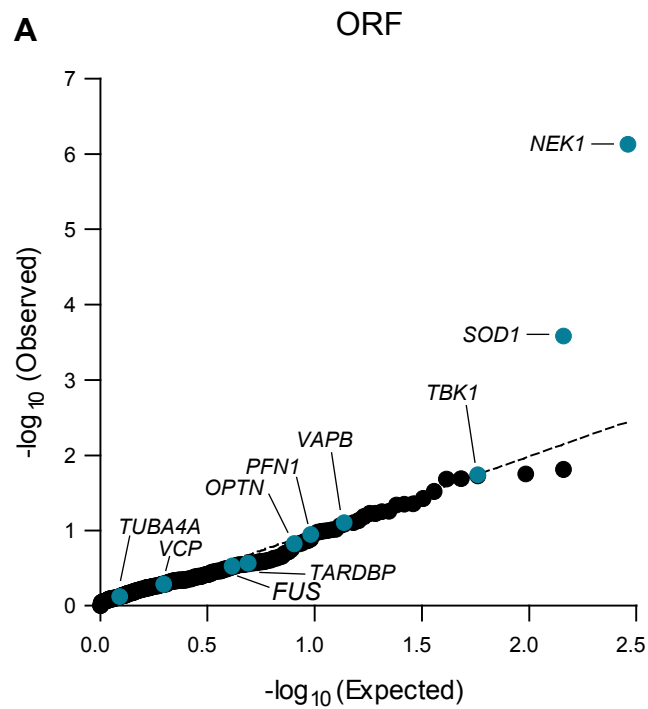


665 **Fig 5. *IL18RAP* 3'UTR variant ameliorates disease in *C9orf72* patient iMNs and in patients with**
666 **ALS.** Experimental setup: Time-lapse survival tracking microscopy of *Hb9*::RFP+ iMNs, transduced
667 with *IL18RAP* lentiviruses, after neurotrophic factors withdrawal and introduction of IL-18 cytokine
668 **(A).** Kaplan-Meier survival plots for control (CTRL) and *C9orf72* patient (C9-ALS) iMNs, with wild-
669 type (WT) *IL18RAP*, *IL18RAP* harboring variants in the 3'UTR (V3, V1) or an *IL18RAP* dominant
670 negative coding mutant (E210A-Y212A-Y214A) 3CDS. Traces of iMNs from 2 donors per genotype
671 (control/ C9-ALS lines), quantified from 3 independent iMN differentiation experiments per line.
672 Number of iMNs quantified per treatment denoted. One-sided log-rank test for the entire survival time
673 course **(B-D)** and corresponding hazard ratio of cellular death, relative to C9-ALS iMNs with wild-type
674 *IL18RAP* 3'UTR **(E).** Association of age of death (9 patients with protective 3'UTR variants /4263
675 patients with available phenotypic data in Project MinE and NYGC cohorts **(F)** or diagnosis (8/4216
676 patients) **(G).** *IL18RAP* variant is associated with delayed age of death (+6.1 years, * P<0.05) and age of
677 diagnosis (+6.2 years, subthreshold significance of P = 0.06), relative to the mean age of all Project
678 MinE and NYGC ALS patients. Box plots depicting median, upper and lower quartiles, and extreme
679 points, one-sided Mann-Whitney test. * P<0.05; *** P<0.001.

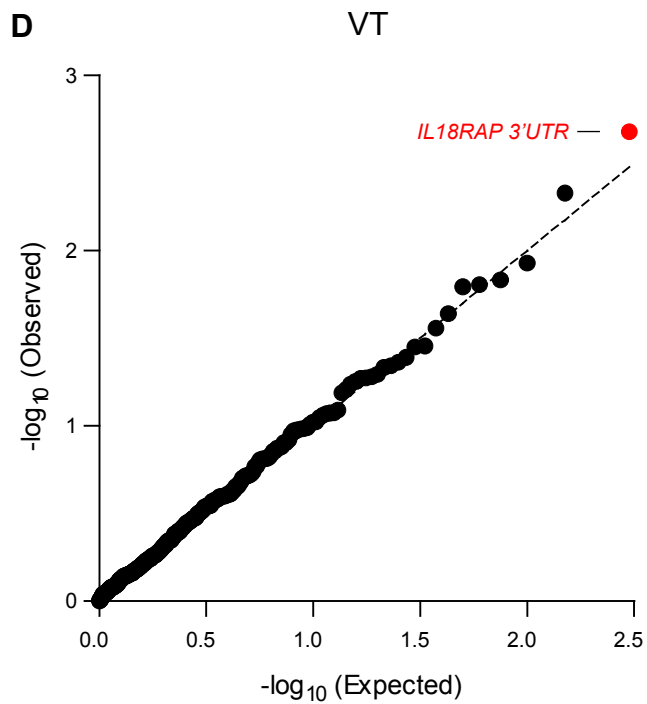
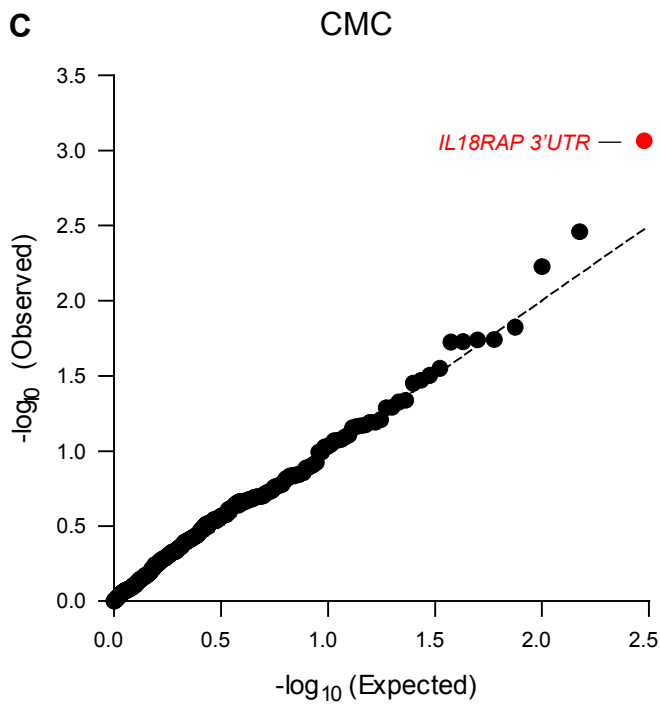
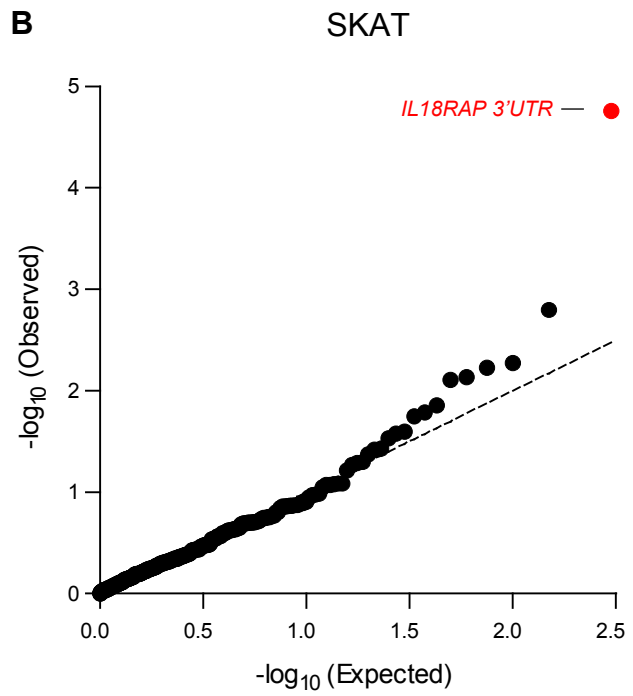
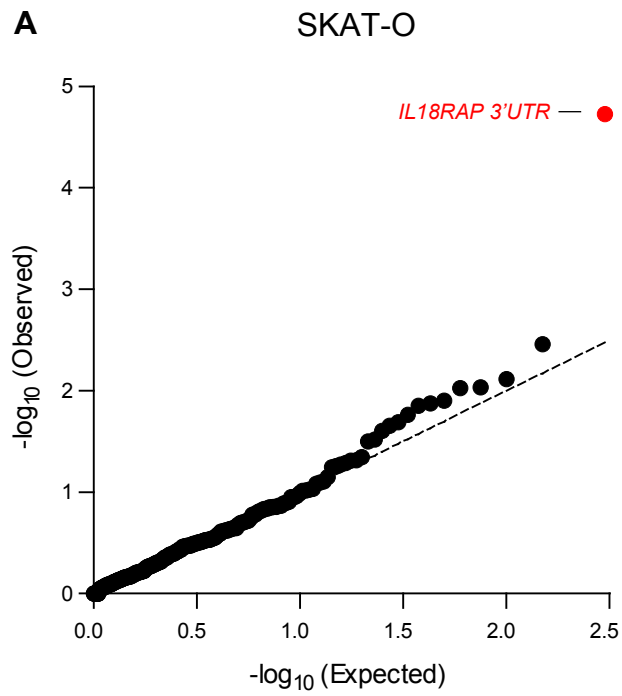
A**B**

Supplementary Fig.1 - Eitan et al. (Hornstein)

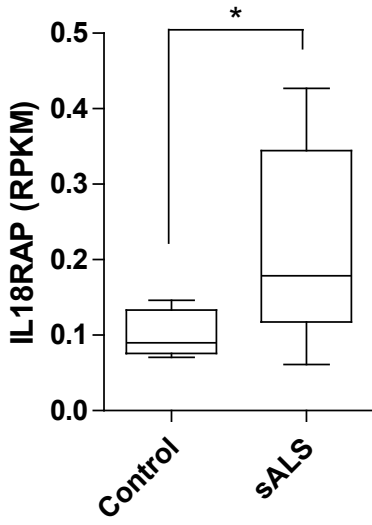
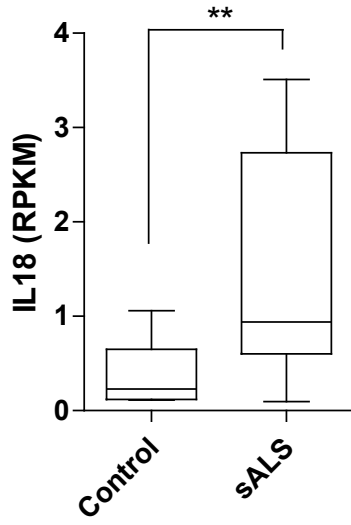
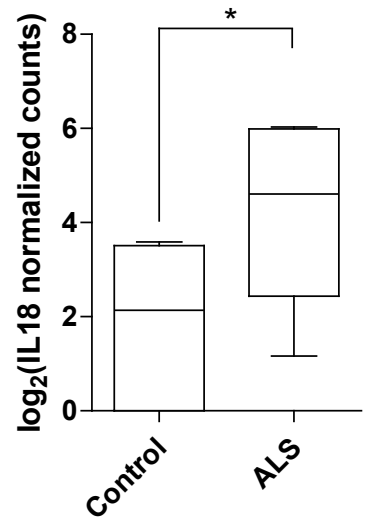
680 **Supplementary Fig. 1. Study design.** (A) Flow chart of approach for discovery of region-based rare-
681 variants in non-coding genomic regions via association studies and (B) diagram depicting regions of
682 interest comprising of 1,750 human pre-miRNA genes, 295 open reading frames encoding for proteins of
683 interest and 295 3'UTRs.



684 **Supplementary Fig. 2. Region-based rare-variant association analyses. (A-D)** QQ plot of obtained
685 and expected P -values for the burden of rare-variants (log scale) gained by collapsed region-based
686 association analysis of different genomic regions, comprised of (A) 295 candidate protein-coding listed
687 in Supplementary Table 3. These ORFs encode for ALS-relevant proteins or proteins that are associated
688 with miRNA biogenesis or activity. Variants were depicted if predicted to cause frameshifting, alternative
689 splicing, abnormal stop codon or a deleterious non-synonymous amino acid substitution, in ≥ 3 of 7
690 independent dbNSFP prediction algorithms (genomic inflation $\lambda = 0.97$), (B) All known pre-miRNA genes
691 in the human genome (genomic inflation $\lambda = 1.30$), (C) predicted networks, comprised of aggregated
692 variants detected on a specific mature miRNA sequence and its cognate downstream 3'UTR targets
693 (genomic inflation $\lambda = 1.17$), and (D) variants abrogating or gaining miRNA recognition elements in
694 3'UTRs of same 295 genes listed in Supplementary Table 3 (genomic inflation $\lambda = 1.03$). Data was
695 obtained from 3,955 ALS cases and 1,819 controls (Project MinE). Features positioned on the diagonal
696 line represent results obtained under the null hypothesis. Open-reading frames of 10 known ALS genes
697 (blue). *IL18RAP* 3'UTR miRNA recognition elements (red).



698 **Supplementary Fig. 3. 3'UTR-based rare-variant association analysis, using different algorithms.**
699 **(A-D)** QQ plot of obtained and expected P-values for the burden of rare variants (log scale) gained by
700 collapsed region-based association analysis of genomic regions comprised of 295 3'UTRs listed in
701 Supplementary Table 3, in Project MinE cohort (3,955 ALS cases and 1,819 non-ALS controls). Variants
702 are not restricted to miRNA recognition elements. Features positioned on the diagonal line represent
703 results obtained under the null hypothesis. *IL18RAP* 3'UTR (red) is the most significant 3'UTR associated
704 with ALS, using different algorithms: (A) Optimized Sequence Kernel Association Test, SKAT-O
705 (genomic inflation $\lambda = 0.98$), (B) Sequence Kernel Association Test, SKAT (genomic inflation $\lambda = 0.98$),
706 (C) Combined Multivariate and Collapsing, CMC (genomic inflation $\lambda = 1.27$), (D) Variable Threshold
707 with permutation analysis, VT (genomic inflation $\lambda = 1.07$).

A**B****C**

708 **Supplementary Fig. 4. Evaluation of IL18RAP and IL-18 mRNA expression in motor neurons of**
709 **patients with ALS. (A-B)** mRNA expression of IL18RAP (A) and IL-18 (B), as reads per kilobase million
710 (RPKM), from NGS study of laser capture microdissection–enriched surviving motor neurons from
711 lumbar spinal cords of patients with sALS with rostral onset and caudal progression (n = 12) and non-
712 neurodegeneration controls (n = 9; ⁴³ GSE76220). two-sided Student's t test with Welch's correction on
713 log-transformed data. (C) IL-18 mRNA expression, as log₂-normalized counts, from NGS study of
714 induced ALS motor neurons (n = 4 different donors in duplicates) or non-neurodegeneration controls (n=3
715 different donors in duplicates; ⁴⁴ DESeq analysis). Box plots depicting median, upper and lower quartiles,
716 and extreme points. *P < 0.05; **P < 0.01.